UNISS
UNIVERSITÀ
DEGLI STUDI
DI SASSARI

UNIVERSITY OF SASSARI

DEPARTMENT OF VETERINARY MEDICINE

PhD Course in Veterinary Science

Curriculum: Reproduction, Pathology, Breeding and Animal Welfare

"Standardization of 3D Spheroid Generation and Mass Density Profiling: Development of a Biofluidic Instrument and Application to Ovine Trophoblast Models"

PhD Course Director: Alberto Alberti

Supervisor: Professor Sergio Ledda

PhD Candidate: Davide Piras

Cycle XXXVII

Funding: This work was supported by MISE project, financial number: F/200110/03/X45—CUP B81B19000700008.

A part of this work was published in the: *Biology 2025, 14(10), 1381; https://doi.org/10.3390/biology14101381*

Preface

This thesis was developed within the framework of a research program funded by the Italian Ministry of Economic Development (MISE), dedicated to advancing innovative platforms for three-dimensional cell culture, functional analysis, and biophysical characterization of organoids, with particular emphasis on placental models. The project was carried out through a multidisciplinary consortium composed of CellDynamics, the University of Sassari, the University of Milan, IRCCS San Raffaele, and additional academic and industrial partners, each contributing complementary expertise in cell biology, microfluidics, and advanced imaging technologies.

Within this consortium, CellDynamics served as the technological leader, overseeing the design, optimization, and validation of the CELLviewer microfluidic analysis system. The company provided the engineering expertise required for the development of the measurement platform, the definition of sterilization procedures for microfluidic circuits, the implementation of acquisition workflows, and the processing of analytical parameters used throughout this study.

In parallel, the University of Sassari conducted the biological activities central to the project, focusing on the generation, culture, and analysis of spheroids derived from ovine placental trophoblasts, as well as the evaluation of the effects of nutraceutical antioxidant molecules. The experimental work included the isolation of trophoblast cells from early gestation placental tissue, the standardization of 3D culture systems, the optimization of spheroid aggregation and viability, the acquisition of biophysical parameters using the CELLviewer, and the assessment of cellular responses to chemical stressors.

The synergy between CellDynamics and the University of Sassari represented the operational core of this thesis. On one side, the technological development of the CELLviewer enabled the quantitative and reproducible measurement of mass density, size, and morphological parameters of spheroids. On the other, the biological characterization performed at the University of Sassari validated the platform in complex cellular models, demonstrating its applicability to trophoblast biology and placental organoid research.

The MISE project thus provided an integrated environment in which technological innovation and biological experimentation could mutually reinforce each other. This thesis emerges from this integration, contributing both to the validation of the CELLviewer for use with placental models and reference cell lines, and to the development of innovative strategies for the standardization, short-term transport, and functional characterization of viable spheroids.

Table of Contents

1. Introduction

1.1. Three-Dimensional Cell Culture Systems
1.2. Comparison of 3D Culture Platforms
1.3. Agarose as a Material for 3D Cell Culture
1.4. Short-Term Transport and Cryopreservation of 3D Spheroids
1.5. Mass Density as a Non-Invasive Biophysical Marker for Cell Characterization
1.6. Ovine Models in Reproductive Biology: Trophoblast Spheroids and Oocytes
1.7. Nutraceutical Molecules in Cellular Protection: Verbascoside and Crocetin
1.8. Aim of Research

2. Materials and Methods

2.1. Cell Lines and Primary Cultures
2.1.1. Ovine Fibroblasts
2.1.2. Human Trophoblast Cell Line (JAR)
2.1.3. Primary Ovine Trophoblast Cells
2.1.4. Ovine Oocytes
2.2. Fabrication of Agarose Microstructured Scaffolds
2.2.1. CAD Design of Microwell Geometry
2.2.2. Master Mold Fabrication via SLA 3D Printing
2.2.3. Silicone Negative Mold Preparation
2.2.4. Agarose Casting Procedure
2.3. Generation of 3D Spheroids
2.3.1. Seeding and Aggregation in Agarose Scaffolds
2.3.2. Hanging-Drop Spheroid Generation
2.4. Short-Term Transport System
2.4.1. Agarose Immobilization Procedure
2.4.2. Post-Transport Recovery
2.5. Cryopreservation Procedures: Slow freezing
2.6. Drug and Nutraceutical Treatments
2.6.1. Nutraceutical Treatment of Spheroids Generated in Agarose Scaffolds and Hanging-Drop Cultures
2.6.2. Live/Dead Staining
2.6.3. Alamar Blue Metabolic Activity Assay

2.7. Mass Density Measurements
2.7.1. W8 Analyzer
2.7.2. Prototype Biofluidic Density-Measurement Instrument (CELLviewer)
2.7.3 Validation of the Sterilization Procedure in the Prototype Instrument

2.8. Statistical Analysis

3. Results

3.1. Agarose-Based 3D cell Culture Systems (Figure 1–2)

3.2. Short-Term Transport System (Figure 3)

3.3. Metabolic Profiling of Cryopreserved vs. Transported Spheroids (Figure 4)

3.4. Live/Dead Analysis of Cryopreserved Spheroids (Figure 5)

3.5. Dose–Response Analysis of Nutraceutical Compounds in JAR Cells (Figure 6)

3.6. Establishment of primary ovine trophoblast cultures (Figure 7)

3.7. Metabolic Response of Ovine Spheroids to Nutraceutical Treatment (Figure 8)

3.8. Biophysical Analysis: Mass Density, Weight, and Diameter (Figure 9)

3.9. Live/Dead After Nutraceutical Exposure (Figure 10)

4. CELLviewer Prototype: Fluidic and Functional Architecture (Figure 11–12)

4.1 Sterilization results (Figure 13)

5. Discussion

6. Conclusions

7. Appendix A. Analysis of Ovine Oocytes

8. References

1.1 Three-Dimensional Cell Culture Systems

Traditional two-dimensional (2D) cell cultures have been the foundational technology for in vitro experimentation for over a century. Despite their widespread use, 2D systems present fundamental biological limitations: cells are forced to grow on rigid, flat substrates, lack physiologically relevant cell-cell and cell-matrix interactions, and experience mechanical and biochemical conditions that diverge substantially from those found in living tissues. These constraints alter cell morphology, polarity, gene expression, and metabolic activity, often leading to misleading or poorly translatable results in both biomedical and veterinary contexts [1–3].

The transition from 2D to three-dimensional (3D) cell culture systems represents a major paradigm shift. In 3D environments, cells self-organize into multicellular aggregates commonly known as spheroids that mimic the structural, biochemical, and mechanical microenvironment of in vivo tissues. The emergence of spheroid technology has enabled researchers to recapitulate gradients of nutrients, oxygen, metabolites, and signaling molecules, generating multicellular architectures that reproduce key features such as proliferation zonation, hypoxic cores, extracellular matrix deposition, and tissue-like stiffness [4–6]. These characteristics make spheroids a more physiologically relevant model than monolayers for studying cell survival, differentiation, drug response, and biochemical pathway activation.

The biological advantages of spheroids derive from their three-dimensionality. Cells within spheroids exhibit more realistic cytoskeletal organization, increased expression of adhesion molecules such as E-cadherin and integrins, and enhanced activation of mechanotransduction pathways, particularly those involving YAP/TAZ and focal adhesion complexes [7]. Furthermore, spheroids display higher resistance to chemotherapeutic agents and environmental stressors, reflecting the diffusion barriers and microenvironmental heterogeneity characteristic of real tissues [8]. These properties make 3D models indispensable for drug screening, toxicology, cancer biology, and tissue engineering.

In veterinary science, 3D cultures have gained increasing attention as models that bridge the gap between laboratory experimentation and clinical or agricultural applications. Spheroid-based systems have been used to investigate reproductive biology, placental development, infectious diseases, toxicological assessment, and comparative oncology in species such as cattle, sheep, pigs, horses, and companion animals [9–12]. The ability to culture organ-specific or species-specific cells in physiologically relevant 3D structures allows for improved modeling of unique anatomical and metabolic traits found in veterinary species, which often cannot be reliably replicated using human-derived cell lines.

Moreover, the use of 3D cell culture is particularly advantageous for studying reproductive biology and placentation in ruminants, where cell-cell interactions, trophoblast invasion, and growth factor gradients play essential roles. Spheroids have emerged as a promising in vitro platform for modeling trophoblast behavior, oocyte development, embryo maternal communication, and uterine microenvironment dynamics [13–15]. Their nonanimal, high fidelity format also aligns with the 3Rs principles (Replacement, Reduction, Refinement) that guide ethical animal research.

Overall, 3D culture systems represent a substantial improvement over traditional 2D platforms by offering higher physiological relevance, more predictable responses to biochemical stimuli, and improved translational value across both biomedical and veterinary fields.

1.2. Comparison of 3D Culture Platforms and Current Approaches for 3D Cell Model Generation

A wide array of 3D culture technologies has emerged in the last two decades, driven by the need to reproduce the complexity of living tissues more accurately than classical two-dimensional (2D) systems. While 2D cultures force cells into unnatural geometries and fail to recapitulate biochemical and mechanical gradients, 3D systems recreate cell-cell and cell-matrix interactions, structural heterogeneity, and microenvironmental cues essential for tissue-like behavior. The methods currently used for 3D culture can be broadly classified into scaffold free aggregation systems, scaffold-based hydrogels, and bioreactor assisted dynamic cultures, each offering distinct advantages and limitations.

Among the simplest and most widely adopted scaffold free approaches are ultra-low attachment (ULA) round-bottom plates. In ULA wells, surface chemistries prevent cell adhesion, forcing suspended cells to sediment toward the center of the concave well where they spontaneously aggregate. ULA plates are inexpensive and compatible with high-throughput formats; however, spheroid formation depends strongly on initial seeding density, gravitational sedimentation, and intrinsic cell-cell adhesion strength, often resulting in heterogeneous spheroid sizes and compaction properties [16]. Moreover, the polystyrene substrate is orders of magnitude stiffer than physiological tissue, introducing non-biological mechanical cues [17].

Another classical scaffold-free method is the hanging-drop system, where cells aggregate at the bottom of a suspended droplet due to surface tension and gravity. Hanging-drop cultures can generate highly uniform spheroids and enable precise control of initial cell number. Nonetheless, the method suffers from limited nutrient volume, rapid evaporation, challenges in medium exchange, and low scalability [18]. The absence of a supporting matrix also means that cells experience no mechanical confinement, limiting investigations involving mechanobiology or ECM-dependent signaling.

More recently, microfluidic technologies have enabled droplet-based spheroid generation, in which cells are encapsulated in aqueous droplets suspended in an immiscible oil phase. These droplets serve as micro-reactors that permit controlled aggregation, high reproducibility, and integration with automated workflows. However, droplet microfluidics typically requires surfactants, specialized equipment, and downstream recovery steps that complicate biological handling [19].

Scaffold-based 3D systems

Scaffold-based systems introduce extracellular matrix (ECM) analogues to support cell growth, providing biochemical and mechanical cues missing in scaffold-free cultures.

Hydrogel scaffolds including Matrigel™, collagen, fibrin, gelatin methacrylate (GelMA), and alginate represent some of the most biologically relevant platforms. Matrigel supports organoid growth in many tissues but suffers from batch variability, undefined composition, and strong adhesive properties that interfere with spheroid aggregation. Collagen and fibrin hydrogels allow cells to remodel the matrix, making them excellent for studying migration and invasion but poorly suited for forming uniform spheroids due to variable contraction and degradation [20].

Alginate microcapsules allow encapsulation of cell clusters in mechanically tunable shells produced via ionic crosslinking. While alginate provides excellent diffusion properties and biocompatibility, it is bioinert and requires RGD or other peptide functionalization to promote adhesion, making it less attractive for simple spheroid formation.

Agarose-based scaffolds, in contrast, offer a uniquely inert environment. Agarose neither supports protein adsorption nor cell adhesion, ensuring that aggregation relies solely on controlled cell–cell interactions. Microfabricated agarose microwells including cylindrical, pyramidal, or hexagonal morphologies enable the generation of hundreds of highly uniform spheroids in parallel. The geometry of the microwells dictates the final spheroid size, compactness, and symmetry [21], while the tunable stiffness (1–10 kPa for typical concentrations) makes agarose mechanically closer to soft tissues than polystyrene or glass [22]. This tunability allows the investigator to modulate mechanotransduction through elastic confinement, giving agarose scaffolds a major advantage for studies requiring defined mechanical microenvironments.

Bioreactor-assisted 3D systems

Dynamic 3D systems, such as spinner flasks, rotating-wall vessels, and perfusion bioreactors, enable continuous nutrient exchange, reduced shear stress, and enhanced mass transfer. Spinner flasks generate spheroids through constant agitation, but tend to produce aggregates with variable shapes and sizes. Rotating-wall vessels simulate microgravity conditions, promoting low-shear aggregation and improved tissue organization [23]. Although powerful, bioreactors require specialized equipment, large culture volumes, and considerable optimization, making them less suitable for routine assays.

More advanced systems incorporate microfluidic perfusion, which offers precise control over nutrient gradients, shear stress, and mechanical cues. Microfluidic 3D culture platforms support

long-term growth and dynamic monitoring but remain technically demanding and less accessible for standard laboratory workflows [24].

Role of substrate stiffness and mechanobiology

Across all 3D culture methods, mechanobiology plays an essential role. Cells continuously sense substrate stiffness, confinement, and tension through integrins, focal adhesions, and mechanosensitive pathways such as YAP/TAZ and Rho-ROCK signaling. Stiff substrates promote enhanced cytoskeletal contractility, altered metabolic states, and lineage specification [25]. In contrast, softer hydrogels including agarose limit excessive spreading and maintain cells in phenotypes closer to in vivo states.

Mechanical confinement also shapes internal spheroid architecture, influencing nutrient diffusion, hypoxia gradients, proliferation zones, and matrix deposition. Therefore, selecting a 3D culture method is not merely a technical decision but a determinant of the biological behaviors observed.

1.3 Agarose as a Material for 3D Cell Culture

Agarose is a linear polysaccharide derived from red algae and widely used in biomedical research due to its biocompatibility, mechanical tunability, and inert surface chemistry. Its unique physical and chemical properties make it particularly suitable for three-dimensional (3D) cell culture systems requiring controlled aggregation, non-adhesive substrates, and reproducible microstructural environments. When dissolved in hot aqueous solutions and allowed to cool, agarose forms a physically crosslinked network stabilized by hydrogen bonding, which provides a mechanically stable yet biologically inert hydrogel [26].

One of the key features of agarose relevant to 3D cell culture is its non-adhesive nature. Unlike collagen, fibrin, or Matrigel, agarose does not naturally support protein adsorption or integrin-mediated adhesion, ensuring that cells rely predominantly on cell–cell interactions for aggregation. This property enables highly predictable spheroid formation without the confounding effects of ECM remodeling or substrate-driven spreading [27]. Additionally, agarose gels exhibit high optical transparency, allowing bright-field and fluorescence imaging without significant light scattering, which is essential for long-term monitoring and morphological analysis.

The mechanical properties of agarose can be finely tuned by adjusting polymer concentration. Typical concentrations ranging from 0.5% to 4% (w/v) yield elastic moduli between 0.5 and 20 kPa, comparable to the stiffness of many soft tissues [28]. This tunability allows researchers to explore the influence of mechanical confinement on spheroid compaction,

mechanotransduction pathways, and metabolic adaptation. Importantly, agarose remains stable over extended culture periods and does not degrade enzymatically, ensuring long-term consistency in mechanical and biochemical conditions.

Agarose is also highly amenable to microfabrication, which has enabled the creation of microwell arrays with defined shapes and dimensions. Techniques such as soft lithography, micromolding, laser ablation, and 3D printing of master molds are commonly used to produce microstructured templates that can be cast with molten agarose [29]. By controlling microwell geometry pyramidal, cylindrical, conical, or hexagonal, it is possible to dictate spheroid size, symmetry, and cell number per aggregate. Hexagonal or polygonal wells are particularly advantageous for minimizing bubble entrapment and improving liquid distribution during cell seeding.

Compared to other 3D culture platforms, agarose-based microwell systems offer substantial advantages in experimental standardization and reproducibility. The inert, non-degradable nature of agarose eliminates batch variability common to biologically derived matrices such as Matrigel or collagen. Furthermore, the ability to generate hundreds of uniform spheroids within a single scaffold enhances throughput and reduces experimental noise. Since agarose does not interfere with molecular assays, spheroids can be easily retrieved for downstream analyses including flow cytometry, immunofluorescence, mass density measurements, and transcriptomics.

Overall, agarose combines mechanical tunability, optical clarity, chemical inertness, and microfabrication compatibility, making it an ideal material for scalable and reproducible 3D cell culture especially in applications requiring precise control over spheroid architecture and mechanobiological conditions.

1.4. Short-Term Transport and Cryopreservation of 3D Spheroids

The ability to transport living three-dimensional (3D) cell models between laboratories is increasingly important in biomedical and veterinary research. Spheroids and organoids are now used for drug screening, toxicology, regenerative medicine, and reproductive biology, yet most studies rely on fresh, locally generated 3D cultures. Unlike 2D monolayers, 3D aggregates possess complex microarchitectures, nutrient and oxygen gradients, and unique mechanical properties that can be disrupted by conventional handling. Therefore, ensuring the preservation of viability and structural integrity during transport is essential for enabling collaborative studies and large-scale experimental pipelines.

Traditionally, cryopreservation has been the method of choice for biological storage and shipment. Slow-freezing protocols using dimethyl sulfoxide (DMSO) as a cryoprotective agent (CPA) enable long-term storage at −80 °C or in liquid nitrogen. However, cryopreservation poses significant challenges for 3D systems. Ice crystal formation, CPA-induced cytotoxicity, osmotic shock, and mechanical stresses during thawing disproportionately affect spheroids, whose compact structure and limited diffusion capacity make them more susceptible to injury than single cells or thin monolayers [30–32]. Studies consistently report reduced post-thaw viability, loss of cellular cohesion, and increased apoptosis within spheroid cores, especially in large aggregates or primary cell-derived models [33]. Additionally, thawed spheroids often require long recovery periods before they can be used experimentally, limiting their practicality for rapid deployment.

Because of these limitations, cryopreservation is poorly suited for short-term biological transport (24–72 hours). Many research groups and clinical laboratories require immediate use of 3D models upon arrival, making cryogenic methods requiring CPA removal, viability recovery, and specialized equipment impractical for routine exchanges. Furthermore, shipping samples in liquid nitrogen is expensive, logistically complex, and subject to regulatory restrictions.

To address these challenges, alternative approaches based on non-cryogenic, hypothermic preservation have been explored. In these methods, spheroids are maintained at reduced temperatures (typically 4–20 °C) to slow metabolic activity while avoiding freezing-induced damage. Hypothermic solutions such as UW, HTK, or generic culture media show partial success in maintaining viability, but their effectiveness strongly depends on sample geometry and mechanical stability [34]. While 2D cultures tolerate hypothermic transport reasonably well, spheroids tend to suffer from dehydration, mechanical deformation, and nutrient depletion unless embedded in a supportive matrix.

For this reason, gel-based and semi-solid systems have gained attention. Hydrogels such as alginate, gelatin, and agarose can physically stabilize spheroids, reduce mechanical stress during movement, and create a controlled microenvironment with slower diffusion and improved moisture retention [35]. Among these, agarose is particularly promising due to its non-adhesive properties, mechanical stability, and ability to form conformal protective layers around 3D aggregates. Its thermal gelation allows spheroids to be gently immobilized without chemical crosslinkers, offering a simple strategy for short-term preservation and safe transport.

Despite progress, no standardized, widely adopted system exists for shipping viable spheroids over short timeframes. Most laboratories still rely on ad hoc solutions, such as transporting spheroids in loosely filled culture plates or embedding them in unstandardized hydrogels. There remains a clear need for a reproducible, mechanically stable, and CPA-free method capable of preserving spheroid morphology, viability, and biomechanical characteristics during transport.

1.5. Mass Density as a Non-Invasive Biophysical Marker for Cell Characterization

Mass density the ratio between cellular mass and volume is an intrinsic physical property that reflects the structural and biochemical state of cells. Unlike molecular markers that depend on specific pathways or gene expression patterns, density integrates multiple aspects of cellular physiology, including macromolecular composition, cytoplasmic crowding, osmotic balance, and organelle content. As such, it represents a global biophysical marker sensitive to changes in cell health, metabolic activity, and structural integrity [36]. In recent years, mass density has emerged as a promising quantitative parameter for assessing 3D cellular systems, where traditional 2D assays often fail to capture internal heterogeneity and biomechanical changes.

The conceptual relevance of density lies in its connection to macromolecular crowding, a fundamental determinant of biochemical reaction rates. Variations in protein, lipid, and nucleic acid content alter cytoplasmic density, influencing enzymatic efficiency, signaling pathways, and stress responses [37]. When cells undergo apoptosis, necrosis, or metabolic suppression, intracellular water content often increases, leading to reduced density. Conversely, highly proliferative or metabolically active cells may display elevated density due to increased biosynthetic activity and cytoskeletal reinforcement.

A wide variety of techniques has been developed to measure density at the single-cell or aggregate level. Quantitative phase imaging (QPI) infers density from refractive index variations but is limited by optics, sample thickness, and the need for transparent tissues [38]. Density-gradient centrifugation can separate cell populations based on buoyant density but lacks the resolution to analyze small differences or intact 3D structures. Suspended microchannel resonators (SMRs) enable high-precision mass and density measurements at the single-cell level but are low-throughput and incompatible with large aggregates such as spheroids [39]. The W8 analyzer, currently one of the few commercial instruments for spheroid density measurement, evaluates terminal velocity in a controlled fluidic column, estimating mass density through Stokes' law. While effective, this method is limited by sample size constraints, measurement noise in large spheroids, and susceptibility to user-dependent variability [40].

Mass density exhibits strong correlations with viability and metabolic activity. Studies demonstrate that spheroids with high metabolic rates tend to be denser, reflecting increased macromolecular synthesis and compact extracellular matrix deposition. In contrast, decreased density is associated with hypoxia, mitochondrial dysfunction, or cytotoxic exposure [41]. Density also correlates with mechanical properties, such as stiffness and compaction, linking biochemical and physical signatures of cell state.

Importantly, density is highly informative for 3D cell models, where gradients in oxygen, nutrients, and waste products create spatially heterogeneous microenvironments. In spheroids, central regions often display lower density due to hypoxic stress, while peripheral proliferative layers exhibit higher density. Changes in density can therefore reveal subtle structural or metabolic alterations that traditional viability assays (e.g., ATP quantification or resazurin reduction) may not detect [42]. For large aggregates or models with complex architectures such as trophoblast spheroids or early-stage organoids mass-density analysis provides a non-destructive, quantitative metric that captures functional and mechanical status simultaneously.

Given its sensitivity, integrative nature, and applicability to intact 3D constructs, mass density represents a valuable readout for assessing spheroid health, treatment response, and preservation quality. Its adoption in veterinary and reproductive research remains limited, highlighting the need for improved analytical tools capable of handling diverse 3D structures, from compact tumor spheroids to fragile oocytes.

1.6 Ovine Models in Reproductive Biology: Trophoblast Spheroids and Oocytes

The ovine species has long been recognized as a highly valuable model in veterinary and reproductive biology due to the structural and functional similarities between sheep and human placentation, the accessibility of reproductive tissues, and the translational relevance of ruminant pregnancy physiology. Unlike rodents, sheep possess an epitheliochorial placenta characterized by restricted trophoblast invasion, unique maternal-fetal signaling pathways, and species-specific mechanisms of nutrient transport, making them an important model for studying early embryonic development, implantation, and placental pathophysiology [43,44].

Three-dimensional (3D) trophoblast models have emerged as powerful tools for investigating placental biology because they recapitulate key morphological and functional features of in vivo trophoblast aggregates. In contrast to monolayers, trophoblast spheroids exhibit physiologically relevant polarization, hormone secretion patterns, extracellular matrix deposition, and differentiation states. Several studies have demonstrated that trophoblast-derived spheroids can mimic early stages of implantation, exhibit appropriate invasive behavior, and respond to inflammatory, hormonal, or metabolic stimuli in a manner consistent with in vivo observations [45,46]. While most 3D trophoblast research has focused on human cell lines such as JAR, BeWo, or HTR-8/SVneo, the application of 3D approaches to ovine trophoblasts remains limited despite its clear potential for advancing veterinary reproductive science.

The generation of primary ovine trophoblast spheroids presents several advantages. These aggregates maintain species-specific behaviors, including ruminant-specific signaling pathways, responsiveness to maternal cytokines, and distinctive adhesion dynamics at the maternal-fetal

interface. Furthermore, ovine trophoblast spheroids enable the study of environmental and nutraceutical compounds relevant to livestock management, offering a controlled in vitro platform for assessing reproductive toxicity, placental function, and embryonic development without the ethical and logistical burden of in vivo experimentation [47].

Similarly, ovine oocytes represent an essential model for reproductive biotechnology. Their biomechanical and biophysical properties, including zona pellucida elasticity, cytoplasmic density, and mitochondrial distribution, are key determinants of developmental competence. Mass density has been shown to correlate with oocyte maturation stage, cytoplasmic organization, and metabolic fitness, making it a promising parameter for non-invasive quality assessment [48]. Given the challenges associated with in vivo ovine reproduction studies, an integrated biophysical approach combining 3D trophoblast models and oocyte density measurement provides a powerful system for exploring reproductive physiology, embryo-maternal communication, and fertility-modulating interventions.

Despite their relevance, standardized protocols for generating, preserving, and analyzing ovine 3D reproductive models are still lacking.

1.7. Nutraceutical Molecules in Cellular Protection:Effect of Verbascoside and Crocetin

In recent years, growing attention has been directed toward nutraceutical compounds with antioxidants, anti-inflammatory, and cytoprotective activity, particularly for their potential applications in supporting cellular homeostasis and mitigating stress induced damage in vitro. Among these bioactive molecules, verbascoside and crocetin have emerged as two of the most studied natural compounds due to their pleiotropic biological properties.

Verbascoside, a phenylpropanoid glycoside commonly found in plants of the genera *Verbascum*, *Plantago*, and *Buddleja*, exhibit strong free radical scavenging capacity and modulates key intracellular pathways involved in oxidative stress responses, such as the Rac-1/HIF-1α axis. Several studies have demonstrated its ability to attenuate ROS production, reduce lipid peroxidation, and exert protective effects on different cellular models exposed to chemical or inflammatory stressors [55–57].

Crocetin, an apocarotenoid derived from saffron (*Crocus sativus*), has likewise been shown to display broad antioxidant and anti-proliferative effects. Its lipophilic nature enables efficient cellular uptake, where it modulates mitochondrial function, enhances the antioxidant defense system, and promotes survival under conditions of metabolic or oxidative challenge. In addition, crocetin has been investigated for its capacity to improve mitochondrial respiration, inhibit apoptosis through modulation of caspase activity, and positively influence the metabolic activity of stem cells and tumor-derived spheroids [58–60].

The relevance of these nutraceutical agents in the context of 3D trophoblast and placental models lies in their potential to modulate oxidative stress, a central factor in placental dysfunction, impaired trophoblast invasion, and altered organoid physiology. Their incorporation into experimental workflows may therefore provide valuable insights into mechanisms of cytoprotection and help identify compounds capable of counteracting stress-induced damage during culture, manipulation, or transport of sensitive 3D cellular constructs.

1.8. Aim of research

The overarching goal of this doctoral project is to establish a complete and coherent technological and biological pipeline for the generation, preservation, and biophysical characterization of three-dimensional (3D) cellular models relevant to veterinary science. This work moves from material design to biological application, integrating agarose-based microstructured scaffolds, short-term preservation strategies, and novel microfluidic technologies to create a unified framework capable of producing robust, transportable, and quantifiable 3D cell systems.

To achieve this, the project focuses first on the development and optimization of agarose-based platforms designed to generate controlled and reproducible spheroids across multiple cell types by exploiting tailored microarchitectures and defined biomechanical properties. Building upon this foundation, the work seeks to establish a short-term transport methodology centered on agarose, capable of maintaining the structural and functional integrity of living spheroids for 24–72 hours without the use of cryoprotectants, thereby enabling reliable inter-laboratory exchange of viable 3D cultures.

In parallel, the project aims to investigate cellular mass density as a quantitative biophysical marker that reflects viability, metabolic state, and structural organization within 3D models. This includes laying the groundwork for density-driven analytical approaches in veterinary cell biology. To support such analyses, a new microfluidic-based instrument for label-free mass density measurement is designed, built, and validated, addressing the limitations of existing commercial systems and expanding analytical capabilities.

Finally, the technologies developed throughout this project are applied to ovine reproductive models including trophoblast-derived spheroids and oocytes to demonstrate their biological relevance, sensitivity, and translational value. Together, these objectives define a research trajectory that unifies material engineering, microfluidics, and veterinary cell biology into a single methodological ecosystem. The outcome is a validated set of tools and concepts enabling

reproducible production, short-term preservation, and biophysical assessment of 3D cellular systems, advancing both technological innovation and biological understanding in the field.

2. Materials and Methods

2.1. Cell Lines and Primary Cultures

2.1.1 Ovine Fibroblasts isolation

Primary fibroblast cultures were obtained from adult sheep ear tissue collected at a regular slaughter facility. Briefly, each biopsy was washed in 70% ethanol, followed by two washes in phosphate-buffered saline (PBS) and two washes in Dulbecco's Modified Eagle's Medium (DMEM/F-12) containing 1% penicillin–streptomycin–amphotericin B. The biopsies were then cut into ~1 mm fragments using a scalpel and placed in a 60 mm tissue culture Petri dish with 1 mL of fetal bovine serum (FBS). The dish was incubated at 37 ◦C with 5% CO2. After 24 h, the serum was removed and replaced with DMEM/F-12. After 5 days, the tissue fragments were discarded, and the cells that had migrated from the tissue were cultured until reaching 80% confluence. Cells were then detached with 0.25% trypsin and transferred to 75 cm2 flasks, maintained up to the sixth passage.

2.1.2. Human Trophoblast Cell Line (JAR)

The human choriocarcinoma-derived trophoblast cell line JAR was purchased from American Type Culture Collection (ATCC), and cultured under standard conditions (37 °C, 5% CO_2). Cells were maintained in routine monolayer culture and subcultured at ~80% confluence. Prior to spheroid generation, cells were detached, washed in complete medium, and counted. This cell line was used as a reference trophoblast model for comparison with primary ovine trophoblast spheroids.

2.1.3 Primary Ovine Trophoblast Cells

Primary trophoblast cells were obtained from biopsies collected from early ovine placentas, carefully excised while avoiding major blood vessels. Tissue samples were washed five times in phosphate-buffered saline (PBS) supplemented with antibiotics and antimycotics to reduce microbial contamination.

The cleaned biopsies were then subjected to enzymatic digestion using 0.25% trypsin and 0.05% EDTA for 20 minutes at 37 °C to promote tissue dissociation. The resulting suspension, including partially digested tissue fragments, was transferred into T25 culture flasks and maintained under standard culture conditions to allow cell attachment and outgrowth.

During the initial culture phase, residual tissue fragments were intentionally retained, as they served as anchoring points for cellular outgrowth and facilitated the formation of new adherent cell layers. After the first expansion phase, adherent cells were detached using trypsin-EDTA and the suspension was filtered to remove remaining tissue debris. Cells were subsequently replated to obtain a more homogeneous trophoblast-enriched population.

In culture, cells displayed an epithelial-like morphology and tended to organize into clearly distinguishable adherent colonies (“islands”), a growth pattern consistent with trophoblast-like primary cultures described in the literature. For spheroid formation, expanded cells were detached, pelleted, and resuspended at controlled densities optimized for uniform aggregation in agarose microwells.

2.1.4. Ovine Oocytes

The ovaries were recovered from adult sheep 2-6 years, regularly slaughtered. After collection the ovaries were placed in a balanced saline solution (Dulbecco Phosphate Buffer Saline, PBS) supplemented with penicillin / streptomycin 1% at 38 ° C; the transport time from the time of collection to arrival in the laboratory was approximately 1 hour; after washing twice in PBS, the ovaries were dissected for follicle isolation (scraping). These operations were carried out under a horizontal laminar flow biological hood. Oocytes were recovered by rupture of the follicular walls with an 18-gauge needle in a petri dish containing dissection medium consisting of TCM 199 with 25mM Hepes (N-2-Hidroxyethylpiperazina-N-2 ethansulfonic Acid) to stabilize the pH, (streptomycin/penicillin 50mg/ml). The selection of oocytes of groups C +, C-, was performed based on the morphological characteristics .

The oocytes destined for maturation were selected on the selection bases of the C + group, therefore for the presence of at least 4 layers of granulosa cells, uniform ooplasm, homogeneous distribution of the lipid component within the cytoplasm and an external diameter of at least 100 µm. At the end of the collection, the oocytes were washed three times in TCM 199 to eliminate traces of follicular fluid. At this point, the oocytes of the C + and C- groups were mechanically decumulated from the granulosa cells, resuspended in 7 ml of W8 analysis solution (CellDynamics) and analyzed at the W8 Physical Cytometer (CellDynamics).

The oocytes of the MII group were incubated in maturation medium (TCM 199 containing 10% of SPE, penicillin/streptomycin 50mg/ml, pituitary gonadotropins LH and FSH (0.1 IU/ml) (Pergonal

Serono) cysteamine 100 µM and estradiol). for the completion of meiosis. The maturation system consisted of 0.5. ml of medium in a four well Nunc plate for cell culture covered with liquid paraffin in which the cumulus-oocyte complexes were cultured for 24h at 38.5°C, at 5% CO2, for 24h. After maturation the oocytes were mechanically decumulated from the granulosa cells, resuspended in 7 ml of W8 analysis solution (CellDynamics) and analyzed at the W8 Physical Cytometer (CellDynamics). The whole experiment was repeated 3 times. Data are expressed as mean ± SD. Statistical analysis was performed using two-tailed unpaired Student's t-test. The cut-off value of significance is $p < 0.05$.

2.2. Fabrication of Agarose Microstructured Scaffolds

2.2.1. CAD Design of Microwell Geometry

The microstructured scaffold was designed using Onshape CAD software (Onshape Inc., USA). The structure consisted of a circular disk with a diameter of 28 mm, sized to fit securely at the bottom of a standard 6-well plate. The disk incorporated 212 inverted-pyramidal microwells arranged in a hexagonal array to maximize spatial efficiency while ensuring uniform spacing between adjacent wells. Each microwell was characterized by a hexagonal base with an edge-to-edge distance of approximately 1.7 mm and a depth of 2 mm. The profile followed an inverted-pyramid geometry, which facilitated bubble escape and promoted uniform cell sedimentation toward the bottom of the well. The microstructured region of the disk was surrounded by perimetric containment walls with a height of 5 mm, designed to retain the cell suspension during seeding. The use of a hexagonal base was specifically chosen to reduce bubble entrapment, as the sharp angles act as capillary escape pathways and prevent the formation of stable gas–liquid interfaces inside the microwells.

2.2.2. Master Mold Fabrication via SLA 3D Printing

The CAD model was exported in STL format and printed using an Elegoo Saturn Ultra SLA 3D printer with a nominal resolution of 0.03–0.05 mm. A high-detail resin suitable for mold fabrication was employed to ensure accurate replication of the microwell geometry. After printing, the master was washed in isopropanol to remove uncured resin residues and then post-cured under UV light for 10–15 minutes to complete polymerization. The printed master was subsequently inspected under stereomicroscopy to verify the fidelity of the microwell features and to exclude the presence of print artefacts such as layer defects or incomplete

edges. Once validated, this master mold served as the template for producing flexible negative molds in silicone.

2.2.3. Silicone Negative Mold Preparation

Negative molds were fabricated using a two-component silicone elastomer (GLS-50, Prochima, Italy). Components A and B were mixed at a 1:1 ratio according to the manufacturer's instructions, ensuring homogeneous blending. The liquid silicone mixture was then poured over the 3D-printed master placed in a sterile Petri dish. To eliminate trapped air and avoid bubble defects in the microstructured regions, the assembly was degassed under vacuum for 5–10 minutes. The silicone was allowed to cure at room temperature for 24 hours. After complete curing, the silicone mold was carefully peeled away from the master and inspected visually and under stereomicroscopy. The intrinsic flexibility of the cured silicone allowed easy demolding of agarose scaffolds in subsequent steps without structural deformation of the microfeatures.

2.2.4. Agarose Casting Procedure

Agarose scaffolds were produced using 2.5% (w/v) standard molecular biology–grade agarose (Thermo Fisher Scientific). Agarose powder was dissolved in deionized water and heated until fully melted. The molten solution was then allowed to cool to approximately 60–65 °C to reduce condensation and avoid premature gelation upon contact with the mold. The warm agarose solution was gently poured into the silicone negative mold positioned on a sterile, temperature-resistant surface, taking care to fill the microstructured area uniformly. The mold was left undisturbed at room temperature for 15 minutes to allow complete gelation. Once solidified, the agarose disk was carefully removed from the silicone mold using sterile forceps, and placed in a bottom of standard 6-well plates.

Scaffolds were then equilibrated with pre-warmed culture medium at 37 °C for approximately 15 minutes. Immediately before seeding, the excess medium was carefully aspirated, leaving the microwell region just covered. This procedure ensured correct alignment of the microwells and stable positioning throughout cell sedimentation, and subsequent culture steps.

2.3. Generation of 3D Spheroids

2.3.1. Seeding and Aggregation in Agarose Scaffolds

For spheroid generation, each cell type was first expanded under conventional 2D culture conditions until reaching approximately 80% confluence. Cells were detached using trypsin–EDTA or, where appropriate, a non-enzymatic dissociation buffer, then collected and centrifuged at 300 × g for 5 minutes. The resulting pellet was resuspended in complete culture medium. Cell viability was assessed via trypan blue exclusion, and only suspensions with a viability of at least 90% were used for 3D culture. Depending on the target spheroid size and the specific cell type, the cell suspension was adjusted to final concentrations typically ranging from 3.0×10^5 to 5.0×10^5 cells/mL, corresponding to approximately 1500-2500 cells per microwell.

Prior to seeding, agarose scaffolds were equilibrated for 15 minutes in pre-warmed complete medium and the excess liquid was carefully removed. The cell suspension was then gently dispensed across the entire surface of the agarose disk using a P1000 pipette, ensuring that all microwell regions were uniformly covered. The total volume applied was usually between 500 and 1000 µL. To facilitate uniform sedimentation of cells into the microwells, the plate was left undisturbed in the biosafety cabinet for 5–10 minutes, allowing initial cell settling. Subsequently, the plate was transferred to a humidified incubator at 37 °C with 5% CO_2 for an additional 20–30 minutes to complete sedimentation. Under these conditions, cells entered each microwell primarily by gravity, Following cell sedimentation, complete medium was added gently to avoid disturbing the forming aggregates. Typically, 4–5 mL of medium were introduced along the sidewall of the well, allowing the liquid to rise slowly over the agarose disk without generating turbulent flow. Culture medium was renewed every 48 hours, with particular care taken to maintain a smooth laminar flow during aspiration and addition to prevent dislodging the spheroids. The presence of the agarose disk's containment walls ensured that the fluid level remained stable over the microwell region and prevented cell dispersion outside the structured area.

For downstream assays, spheroids were retrieved directly from the agarose surface. The culture medium was first gently aspirated, leaving a thin layer to prevent the gel from drying. The microwell region was then carefully probed with a cut P200 pipette tip, which allowed individual spheroids to be dislodged without excessive mechanical stress. Spheroids were aspirated into the pipette and transferred into sterile tubes or plates prepared for the subsequent experimental procedure. For downstream assays, manipulations were kept to a minimum to preserve spheroid architecture and prevent fragmentation.

2.3.2. Hanging-Drop Spheroid Generation

Spheroids were also generated using the classical hanging-drop method, which relies on gravitational sedimentation and surface tension to promote spontaneous cell aggregation in a suspended microenvironment. Briefly, cells were expanded under standard 2D culture conditions until ~80% confluence, then detached using trypsin–EDTA and resuspended in complete medium at the desired concentration. For all hanging-drop experiments, cell suspensions were adjusted to obtain 2,500 cells per 20–25 µL droplet, matching the initial cell number used for agarose-based aggregation.

Drops were prepared by pipetting 20–25 µL aliquots of the cell suspension onto the inner surface of the lid of a 100 mm sterile Petri dish, ensuring adequate spacing between adjacent drops to avoid coalescence. The dish base was filled with sterile PBS to maintain a high-humidity environment and minimize evaporation during incubation. After positioning the drops, the lid was carefully inverted and placed onto the dish, allowing the hanging droplets to remain suspended by surface tension.

Under these conditions, cells sedimented to the bottom of each droplet and progressively aggregated to form spheroids. Dishes were incubated at 37 °C with 5% CO_2 for up to 72 hours, during which spheroid formation proceeded spontaneously. To maintain drop volume and prevent desiccation, plates were monitored daily, and humidity was restored when necessary by replenishing PBS in the dish base. Culture medium was not replaced during this interval to avoid disrupting drop integrity.

At the end of the aggregation period, spheroids were retrieved by gently washing each droplet with 200–300 µL of pre-warmed medium using a P200 pipette. Formed spheroids were collected into low-adhesion plates or transferred directly into downstream assays, taking care to minimize shear forces during pipetting to preserve their compact architecture.

2.4. Short-Term Transport System

2.4.1. Agarose Immobilization Procedure

After 72 hours of spheroid culture within the agarose scaffold, a transport-stabilization system was established to minimize mechanical stress during simulated shipment. The culture medium was carefully aspirated, leaving a thin residual layer to prevent desiccation. A freshly prepared 2% (w/v) agarose solution, cooled to 37–40 °C, was then gently applied to fully cover the microwells, forming a uniform protective overlay on top of the remaining medium. Once the

agarose had solidified, the entire agarose disk containing the spheroids was transferred into a sterile 50 mL conical tube. A defined volume of complete culture medium was added to maintain scaffold hydration and ensure cellular viability throughout the simulation period. Separate tubes were prepared for each experimental condition, corresponding to the temperatures evaluated (4 °C and 20 °C). All tubes were stored for 72 hours under these defined conditions to reproduce a short-term transport scenario. To replicate realistic transport conditions, sealed vials were placed either in a 4 °C refrigerator to simulate hypothermic shipment or in a 20 °C water bath to simulate room-temperature transport. To mimic the passive mechanical stress typically experienced during shipping or routine laboratory transfer, vials were gently handled once every 24 hours. This step introduced a controlled degree of movement without inducing significant shear forces or agitation.

2.4.2. Post-Transport Recovery of Spheroids

At the end of the transport interval, vials were first equilibrated at 37 °C for approximately 10 minutes without agitation. To recover the spheroids, the protective agarose coating was removed using a scalpel and fine forceps. Because the newly added agarose layer does not strongly adhere to the original scaffold once solidified, its removal was straightforward and uniform across samples. After exposing the underlying microwells, fresh culture medium was added, and spheroids were individually collected using a P200 pipette.

To benchmark the effects of hypothermic transport and agarose immobilization, three main control groups were included in each experiment. Fresh, non-transported spheroids served as baseline controls for morphology, viability, and density. Cryopreserved spheroids, processed by standard slow-freezing in 10% DMSO and subsequently thawed, provided a direct comparison between short-term transport and classical cryopreservation. A third group consisted of spheroids maintained in suspension in medium without agarose immobilization, enabling assessment of the specific contribution of mechanical stabilization by the agarose layer. Together, these controls allowed rigorous comparison between hypothermic transport, cryogenic storage, and unstressed reference conditions.

2.5. Cryopreservation Procedures: Slow freezing

After 72 h of growth, spheroids were collected and resuspended in a freezing solution composed of 90% FBS and 10% DMSO at a final concentration of approximately 200 spheroids mL in 1.5 mL cryovials. Slow freezing was performed using Mr Frosty™ (Thermo Fisher Scientific, Waltham, MA, USA), which provides a controlled cooling rate of ~1 °C min^{-1} when placed in a −80 °C freezer overnight. On the following day, cryovials were transferred to liquid nitrogen (−196 °C) for long-term storage.

After 24 hours in liquid nitrogen cryovials were removed and rapidly thawed in a 37 °C water bath under gentle agitation for 50 seconds. Thawed spheroids then underwent their own 24-hour post-thaw assays in parallel with the 72 hour CTRL endpoint and were subsequently returned to standard culture conditions (37 °C, 5% CO_2).

Following thawing, spheroids were resuspended in 8 mL DMEM/F-12 inside a Petri dish coated with 2.5% agarose to prevent adhesion, and incubated at 37 °C with 5% CO_2.

2.6. Drug and Nutraceutical Treatments

2.6.1. Nutraceutical Treatment of Spheroids Generated in Agarose Scaffolds and Hanging-Drop Cultures

Nutraceutical assays were performed on spheroids generated using two culture systems: agarose microstructured scaffolds and hanging-drop aggregation. Crocetin and verbascoside were first dissolved in dimethyl sulfoxide (DMSO) to prepare concentrated stock solutions and subsequently diluted in complete culture medium to obtain the desired working concentrations, as defined in preliminary dose response experiments. Vehicle control conditions were included in all experiments using culture medium supplemented with the same final concentration of DMSO present in treated samples.

For agarose derived spheroids, primary trophoblast cells were allowed to aggregate for 72 hours within the microwell array. At this time point, the culture medium was completely removed and replaced with fresh medium containing the selected concentrations of crocetin or verbascoside. Spheroids remained in situ within the agarose scaffold throughout the exposure period to ensure homogeneous compound diffusion while preserving structural integrity and minimizing mechanical manipulation.

Each experimental condition was performed using three independent agarose scaffolds, which were considered independent biological replicates.

For spheroids produced using the hanging-drop method, the treatment workflow required additional steps due to the physical constraints of the system. After 72 hours of aggregation, each droplet was gently recovered by rinsing with pre-warmed medium, and the pooled spheroids were collected into sterile 15 mL conical tubes. Samples were allowed to settle by gravity or were centrifuged briefly (80–100 × g for 2 minutes), after which the supernatant was carefully aspirated to remove residual drop medium. The spheroid pellet was then resuspended in complete culture medium supplemented with the corresponding concentration of crocetin or verbascoside.

To maintain the same microenvironmental conditions as the original culture method, spheroids were subsequently re-seeded individually into fresh hanging drops (20–25 µL each), ensuring that each droplet contained a single spheroid and that inter-sample variability was minimized. For each treatment condition, spheroids were distributed across at least three independent Petri dishes, which were considered biological replicates.

Following treatment, spheroids from both systems were incubated at 37 °C and 5% CO_2. Time-course analyses were conducted by collecting samples at the predefined experimental endpoints (3, 6, 24, 48, and 72 hours). For all assays, particular care was taken to minimize shear stress during pipetting, as excessive handling can compromise spheroid compactness and confound metabolic or viability measurements.

2.6.2. Live/Dead Staining

The viability of spheroids was also assessed 24 h after thawing using calcein-AM, propidium iodide (PI), and Hoechst. Briefly, 10 spheroids per groups were incubated with 1 µL of calcein-AM (10 µg/µL; Invitrogen, Waltham, MA, USA), 1 µL of PI (10 µg/µL; Sigma-Aldrich, St. Louis, MO, USA), and 1 µL of Hoechst (10 µg/µL; Thermo Fisher Scientific) for 30 min at 37 °C with 5% CO_2. After incubation, spheroids were transferred onto a microscope slide and viewed under a fluorescence microscope (Leica CTR 6000, Leica Microsystems, Wetzlar, Germany).
.

2.6.3. Alamar Blue Metabolic Activity Assay

2.4. Alamar Blue® Assay
Spheroid viability was evaluated by Alamar Blue® (Thermo Fisher Scientific). Briefly, 10 spheroids per group, were transferred (in triplicate) into a 10% Alamar Blue®/DMEM (phenol-red-free) solution in a 96-well plate and incubated at 37 °C with 5% CO_2 for 4 h. Absorbance was read at 570 and 600 nm on a Spectrostar Nano (BMG Labtech, Ortenberg, Germany), and the percentage

of Alamar Blue® reduction was calculated. Measurements were performed at 24, 48, and 72 h post-thawing.
To calculate the % Reduction of Alamar Blue Reagent using absorbance readings:

$$\% \text{ Reduction of Alamar Blue Reagent} = \frac{(Eoxi600 \times A570) - (Eoxi570 \times A600) \times 100}{(Ered570 \times C600) - (Ered600 \times C570)}$$

Eoxi570 = molar extinction coefficient (E) of oxidized Alamar Blue Reagent at 570nm = 80586
Eoxi600 = E of oxidized Alamar Blue Reagent at 600nm = 117216
A570 = absorbance of test wells at 570nm
A600 = absorbance of test wells at 600nm
Ered570 = E of reduced Alamar Blue at 570nm = 155677
Ered600 = E of reduced Alamar Blue at 600nm = 14652
C570 = absorbance of negative control well (media, Alamar Blue Reagent, no cells) at 570nm
C600 = absorbance of negative control well (media, Alamar Blue Reagent, no cells) at 600nm
Alamar Blue readings were expressed as mean ± SD (n = 3 independent wells per condition)**.** Differences between CTRL and SF at each time-point were analysed with a two-tailed, unpaired Student's *t*-test. Prior to testing, residuals were checked for normality (Shapiro–Wilk).
The significance threshold was set at $p < 0.05$**.** All statistics were performed in GraphPad Prism 8.0**;** significant differences are denoted in the figures by asterisks (*$p < 0.05$, **$p < 0.01$, ***$p < 0.001$).

2.7. Mass Density Measurements

Mass density measurements were performed using two complementary approaches: the commercial W8 analyzer and a custom-developed microfluidic density-measurement instrument. Both systems rely on the principle that the gravitational settling behavior of a particle in a fluid is directly related to its density relative to the surrounding medium. Measurements were carried out on freshly generated spheroids, transported spheroids, cryopreserved samples, and treated trophoblast models to evaluate biophysical changes induced by environmental or pharmacological conditions.

2.7.1. W8 Analyzer

For biophysical measurements, 20 spheroids for each group analyzed were transferred to 15 mL Falcon tubes containing 7 mL of W8 analysis solution (CellDynamics, isrl, Bologna, Italy) and analyzed with a W8 Physical

Cytometer (CellDynamics) at 24, 48, and 72 h post-thaw, according to the manufacturer's instructions. The W8 Physical Cytometer measures size, weight, and mass density of spheroids in sterile conditions.

The W8 is a flow-based "physical cytometer" that measures diameter, weight and mass density on single spheroids as they free-fall through a micro-fluidic analysis channel filled with a liquid of known viscosity (η) and density (ρ1). Contact-free free-fall: A peristaltic pump pulls one spheroid at a time from a Falcon tube into a micro-channel, then stops the flow. The spheroid falls through still fluid, satisfying Stokes' law, so its terminal velocity gives the weight.

Automatic diameter capture: While the aggregate rotates during the 2–3 mm fall, a camera records a burst of brightfield images. The software extracts Feret diameters from every frame and averages them, delivering a sub-micron diameter that is more reliable than a single microscope snapshot.

Mass density: The software combines weight and volume (π d3/6) to output the mass density.

Shear stress is kept to minimum, the peristaltic pump feeds each spheroid slowly and centrally, so the aggregate never contacts the channel walls; once inside the measuring zone, the flow is stopped, eliminating surface shear altogether; and because the circuit is closed and sterile, the spheroids remain viable for any downstream assay.

2.7.2. Prototype Biofluidic Density-Measurement Instrument (CELLviewer)

As part of the MISE project, CellDynamics developed a prototype biofluidic instrument capable of performing label-free mass-density analysis directly within standard 96-well plates U-bottom, overcoming several limitations of the W8 analyzer, particularly with respect to sample throughput, compatibility with culture media, and handling of fragile biological specimens such as spheroids and oocytes.

The instrument integrates a temperature-controlled multiwell stage, maintaining samples at 37 °C throughout the entire measurement workflow, thus preserving physiological conditions and reducing thermal stress. Unlike conventional systems that require dedicated measurement buffers, this prototype operates directly in cell culture medium, ensuring superior preservation of spheroid viability during analysis and enabling the characterization of samples maintained in different media or pharmacological treatments. The fluidic architecture is designed to accommodate up to six independent buffers, allowing seamless switching between culture conditions without manual intervention.

Sample acquisition is performed through a custom microfluidic analysis chip that is automatically positioned above each well via a motorized three-axis movement system (X, Y, Z). Once aligned, the chip gently draws the spheroid into the measurement chamber through the coordinated action of two peristaltic pumps: one aspirates medium and sample, while the second simultaneously dispenses fresh medium into the well. This dual-pump mechanism ensures that the 200 µL working volume of each microwell remains constant, maintaining environmental stability and preventing dehydration or shear-induced deformation of the sample.

A critical aspect of the design process involved selecting the optimal fluidic pathways for the transport of media, buffers, and sterilizing solutions within the instrument. Throughout development, several hardware modifications were introduced to refine the reliability and sterility of the system. These included the integration of automated disinfection protocols capable of sterilizing the entire internal fluidic network from buffer reservoirs to the analysis chip using dedicated solutions without requiring operator intervention. Achieving fully automated sterilization was essential due to the instrument's operation in laminar-flow biosafety cabinets, where maintaining aseptic conditions is crucial, especially when working with live spheroids, organoids, or primary cells.

2.7.3 Validation of the Sterilization Procedure in the Prototype Instrument

To validate the effectiveness of the automated sterilization protocol implemented in the prototype biofluidic instrument, a microbiological challenge test was performed using GFP-positive *Escherichia coli* (10^6 CFU/mL). All standard buffer solutions were replaced with this bacterial suspension in order to deliberately contaminate the internal fluidic network and enable monitoring of potential bacterial persistence. This deliberate contamination was designed to simulate a worst-case scenario, ensuring that the sterilization protocol was tested under conditions of maximal microbial load.

A full experimental simulation was conducted in which the fluidic circuits were filled with the bacterial suspension and the system was operated continuously for 3 hours, reproducing typical measurement workflows. This procedure ensured extensive contact between the microbial suspension and all internal surfaces of the system, including reservoirs, valves, tubing, and the analysis chip.

Immediately before initiating the sterilization cycle, samples were collected from six independent checkpoints distributed along the internal fluidic network, including buffer reservoirs, intermediate fluidic pathways, and downstream analysis zones. Approximately 1 mL of fluid was collected from each sampling point and used as a pre-sterilization control.

The instrument then executed the automated sterilization protocol according to the standard operational procedure. After completion of the sterilization cycle, a second set of samples was collected from the same six checkpoints to evaluate residual microbial contamination.

For microbiological analysis, aliquots from each collected sample were plated onto nutrient-rich agar plates and incubated at 37 °C to allow colony formation. Colony-forming units (CFUs) were subsequently evaluated to determine the presence or absence of viable GFP-positive *E. coli*. The complete absence of detectable CFUs after incubation was considered evidence of successful sterilization of the fluidic network.

All microbiological analyses were performed at the Department of Pharmacy and Biotechnology, University of Bologna. The entire microbiological challenge test was repeated twice to confirm the reproducibility of the sterilization results.

Following this microbiological challenge test, the instrument underwent an additional validation step under biologically relevant conditions. Six buffer reservoirs were filled with DMEM culture medium, and a 96-well U-bottom plate was loaded into the instrument. A complete experimental run was then performed under sterile conditions. At the end of the experiment, samples were again collected from multiple checkpoints within the fluidic circuit including buffer compartments, valves, tubing, and the analysis chip to verify the absence of microbial contamination during normal operational use after sterilization.

2.8. Statistical Analysis

All statistical analyses were performed using GraphPad Prism version 8.0 (GraphPad Software, San Diego, CA, USA). Data are presented as mean ± standard deviation (SD) unless otherwise specified. Normality of the data distribution was assessed using the Shapiro–Wilk test.
For spheroid experiments, each agarose scaffold or Petri dish was considered an independent biological replicate, while individual spheroids represented technical measurements within each replicate. For each experimental condition, three independent biological replicates were analyzed.
Pairwise comparisons between experimental groups were performed using a two-tailed unpaired Student's t-test. Outliers were identified using the Tukey method (1.5 × interquartile range) and were excluded only when attributable to clear technical artifacts.
Statistical significance was defined as $p < 0.05$. In figures, significance levels are indicated as follows: * $p < 0.05$, ** $p < 0.01$, *** $p < 0.001$.

3. Results

3.1. Agarose-Based 3D cell Culture Systems (Figure 1–2)

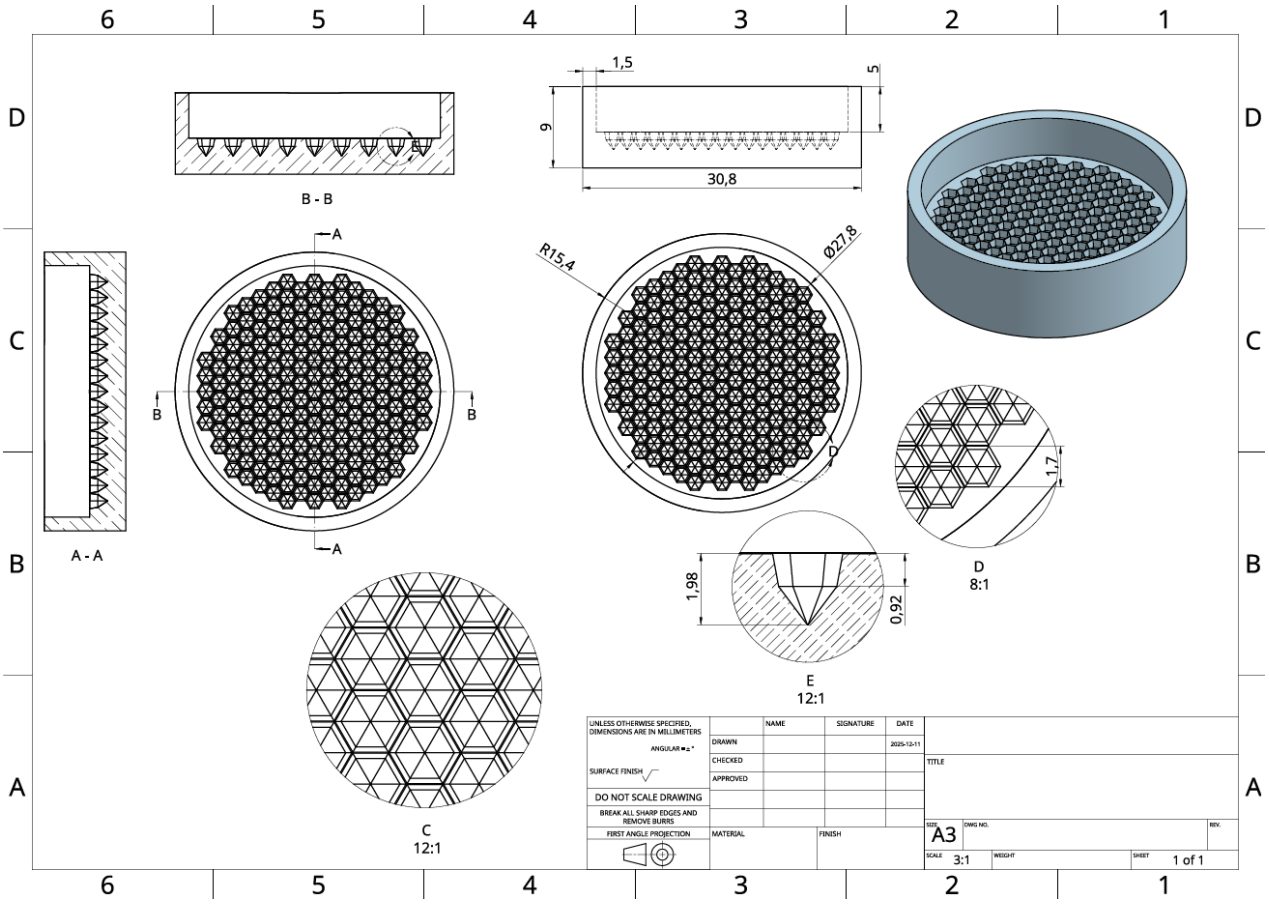

Figure 1.

The technical drawing extracted from Onshape illustrates the cell culture system designed for the generation and maintenance of uniform spheroids. The drawing provides a detailed representation of the geometric layout of the microwells, the overall structure of the device, and the spatial arrangement of its components, while dimensional specifications are reported directly within the figure.

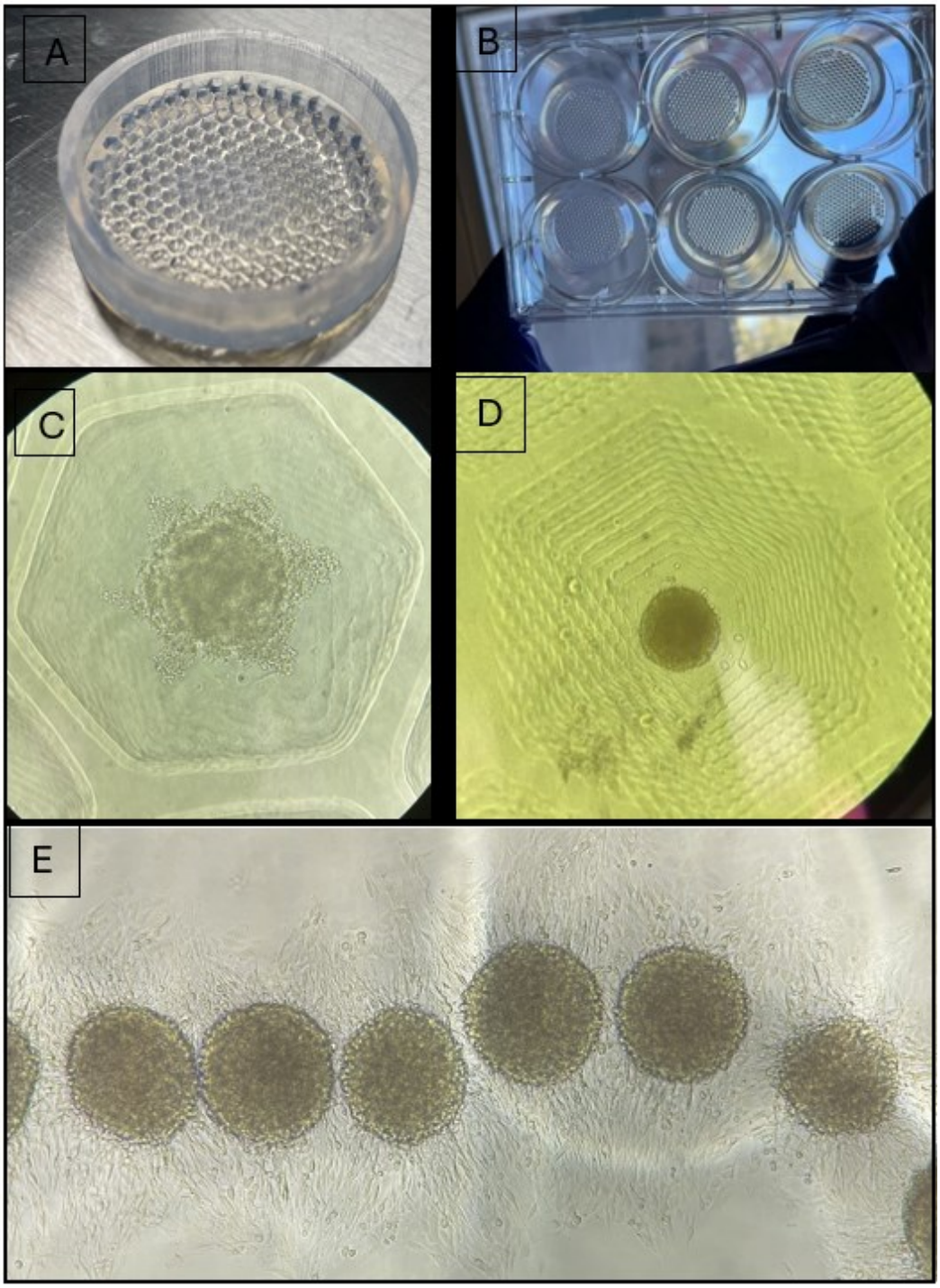

Figure 2.

A. Representative image of the agarose scaffold generated using the silicone mold. **B.** Six-well plate containing six agarose scaffolds prepared for cell seeding. **C.** Microwell at 8 hours after seeding 2,500 fibroblast cells, showing the initial stages of cell aggregation. **D.** Microwell at 24

hours after seeding, displaying a more compact and advanced cellular aggregate. **E.** Spheroids retrieved from the growth system after 7 days and transferred onto a tissue-culture plate for adhesion assays

3.2. Short-Term Transport System (Figure 3)

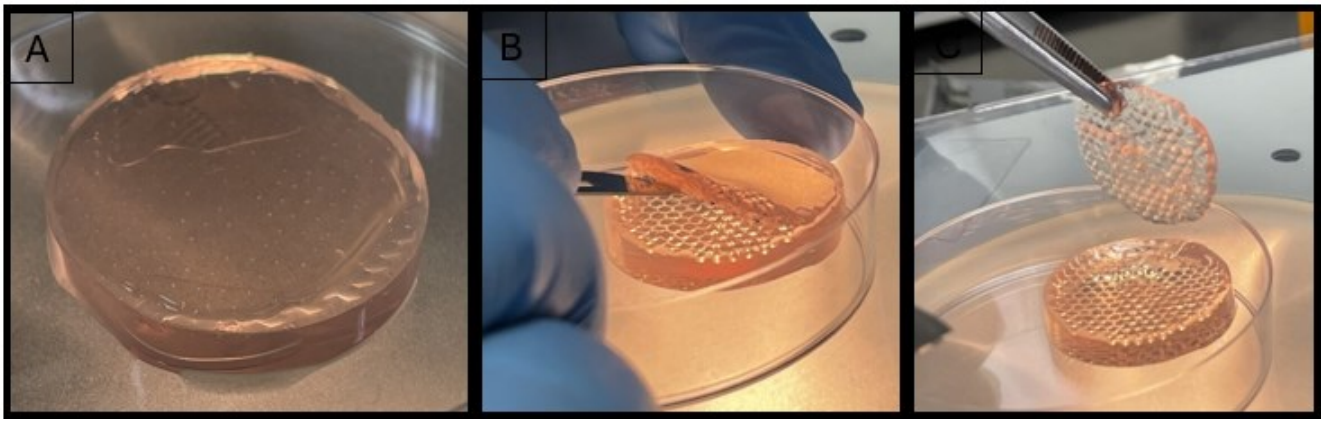

Figure 3.

A. Agarose scaffold containing viable ovine fibroblast spheroids, overlaid with an additional agarose coating for protection during transport. **B.** Initial removal of the agarose coating by making a scalpel incision after 72 hours of transport. **C.** Complete removal of the agarose coating using fine forceps.

3.3. Metabolic Profiling of Cryopreserved vs. Transported Spheroids (Figure 4)

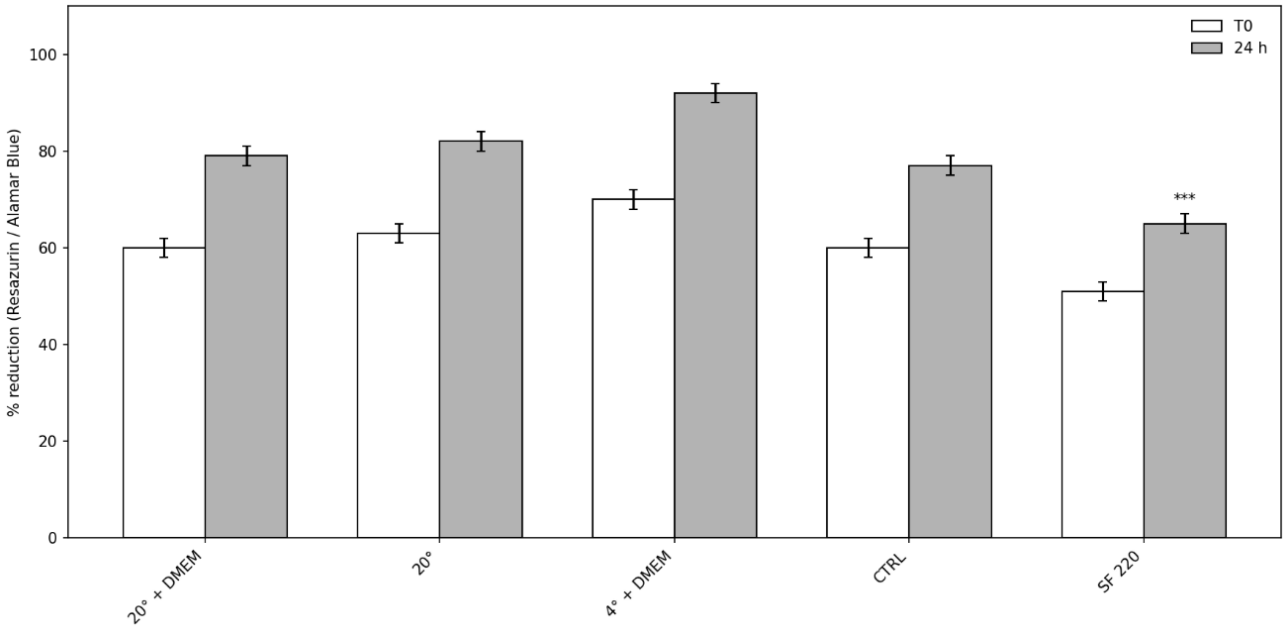

Figure 4. Metabolic activity after thawing. Alamar Blue reduction

Figure 5 shows the percentage reduction of resazurin in the different experimental groups evaluated at two time points (T0 and 24 h). The first three groups represent spheroids subjected to short-term storage under distinct temperature and medium conditions: 20 °C + DMEM, 20 °C, and 4 °C + DMEM. These conditions were included to assess the influence of hypothermic transport parameters on metabolic activity. The following groups, CTRL and SF 220, represent spheroids that were either left untreated (CTRL) or subjected to the short-term freezing protocol (SF 220).

Across all groups, an increase in resazurin reduction is observed from T0 to 24 h, consistent with recovery of metabolic activity after re-equilibration. Among the conditions tested, only the cryopreserved group (SF 220) displayed a statistically significant difference, showing reduced metabolic activity compared to its time-matched control. This indicates that, while hypothermic transport conditions did not markedly impair spheroid viability, the cryopreservation process had a detectable impact on cellular metabolism within the first 24 h post-thaw.

3.4. Live/Dead Analysis of Cryopreserved Spheroids (Figure 5)

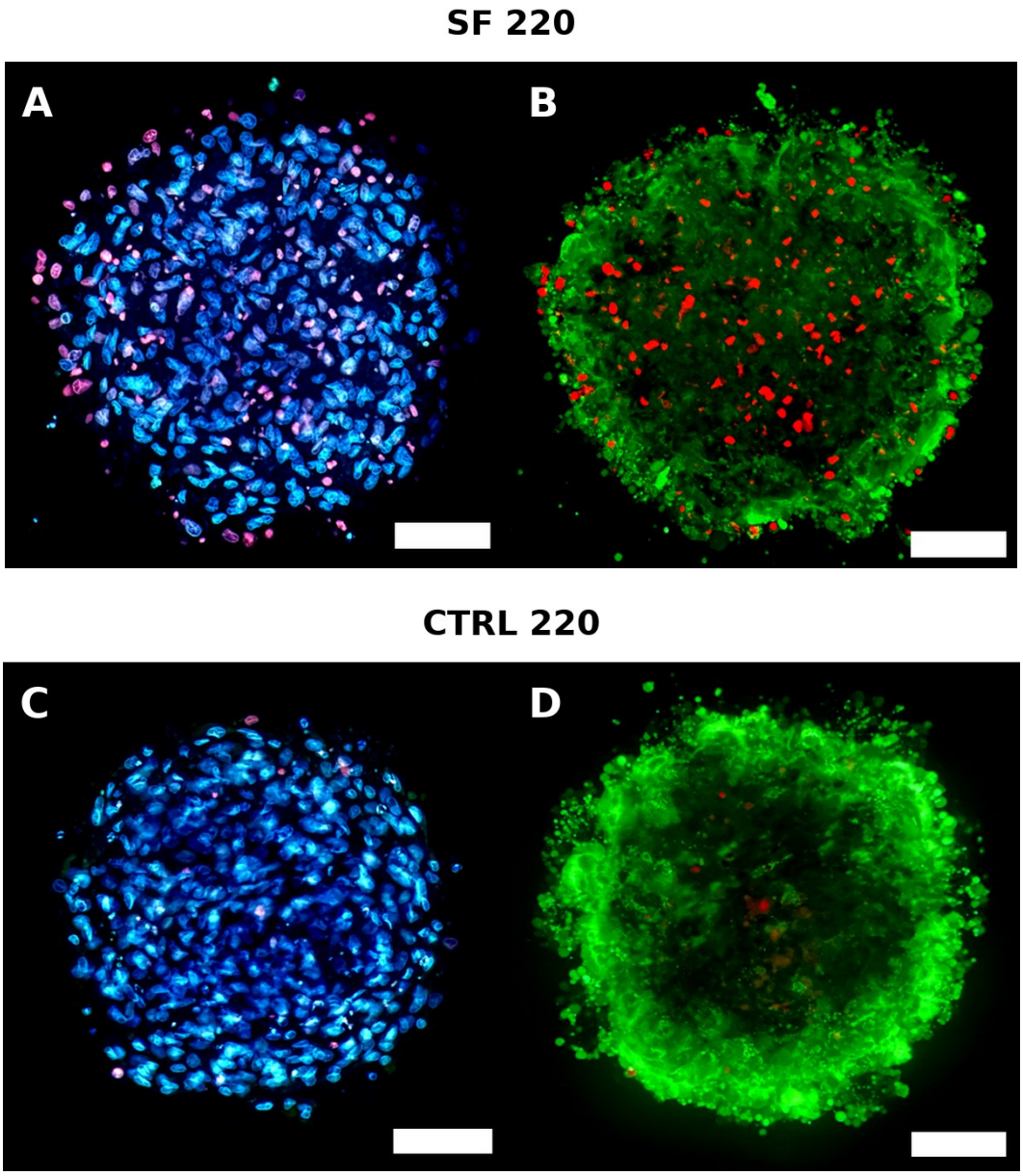

Figure 5. Live/Dead staining 24 h post-thaw. Calcein-AM (green, live cytoplasm) **B-D** , Hoechst 33342 (blue, all nuclei) and propidium iodide (PI, red, dead nuclei) **A-C** in control (CTRL) and slow-frozen (SF) spheroids.
SF-220 shows a higher overall presence of PI-positive cells, indicating increased cellular stress and death. Scale bar = 50 µm.

3.5. Dose–Response Analysis of Nutraceutical Compounds in JAR Cells (Figure 6)

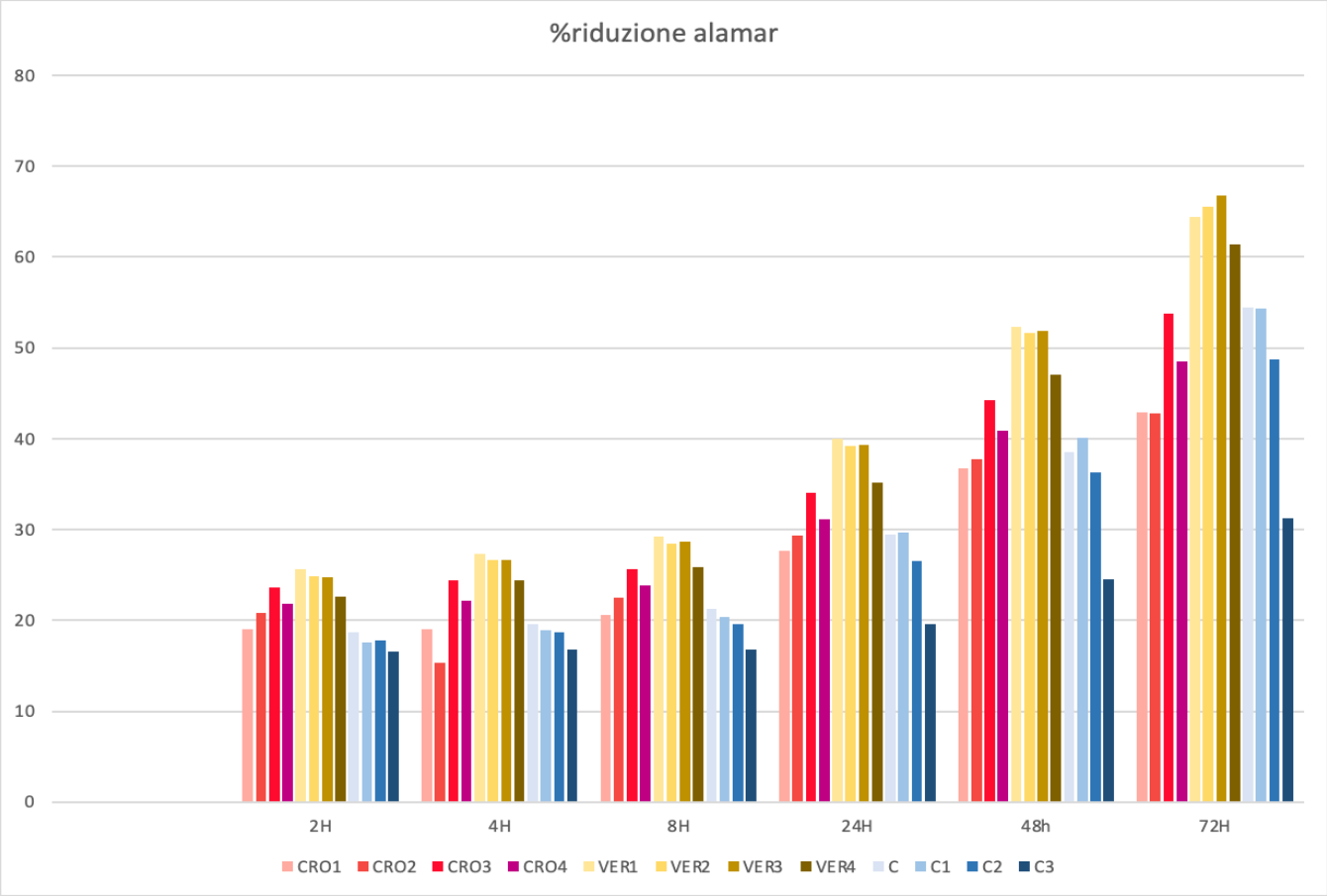

Figure 6.

Time-course Alamar Blue assay for nutraceutical screening on JAR cells.
The graph shows the effect of increasing concentrations of crocetin (Cro1: 13.55 µM; Cro2: 27.1 µM; Cro3: 54.2 µM; Cro4: 108.4 µM) and verbascoside (Ver1: 6.25 µM; Ver2: 12.5 µM; Ver3: 25 µM; Ver4: 50 µM) on the metabolic activity of JAR choriocarcinoma cells, measured by Alamar Blue reduction. Absorbance readings were acquired at 2, 4, 8, 24, 48 and 72 hours after treatment and expressed relative to the untreated control. The time-course curves illustrate how different doses modulate cellular metabolism over short- and mid-term incubation. Among the concentrations tested, Cro3 (54.2 µM) for crocetin and Ver3 (25 µM) for verbascoside exhibited the most favourable profile, sustaining or enhancing Alamar Blue reduction over time without signs of overt loss of viability. On the basis of these screening data, Cro3 and Ver3 were selected as working concentrations for subsequent experiments on ovine placental spheroids.

3.6. Establishment of primary ovine trophoblast cultures (Figure 7)

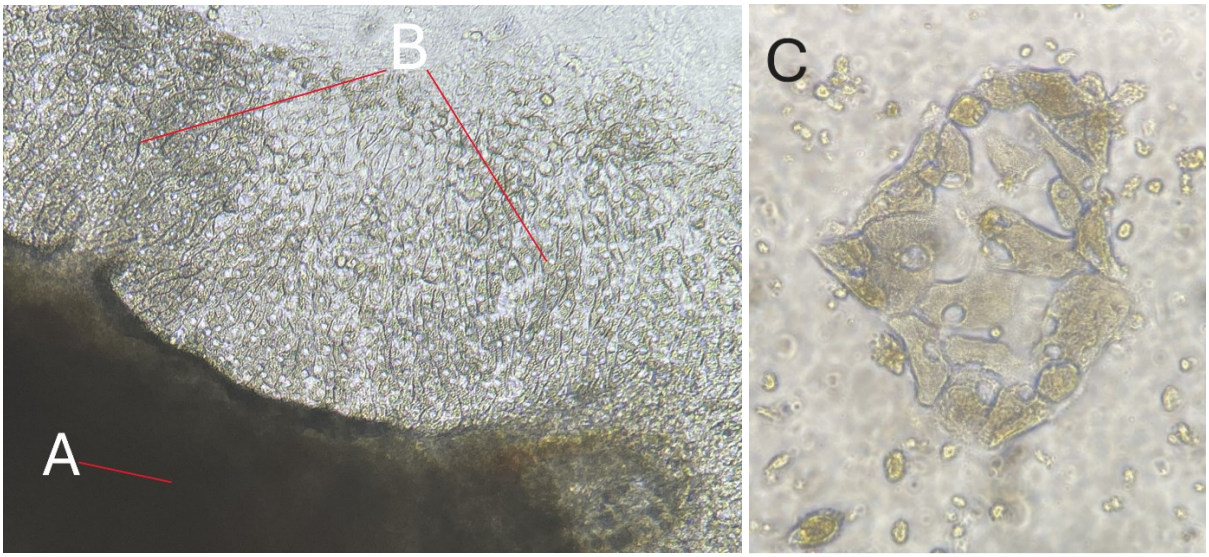

Figure 7.

A.Representative image of placental biopsy fragments after plating in a T25 culture flask. The dark structure corresponds to an adherent placental tissue fragment that serves as a substrate for cellular outgrowth during the initial phase of primary culture establishment.

B.Outgrowth of trophoblast-like cells migrating and proliferating from the placental fragment. Cells display an epithelial-like morphology and progressively expand from the tissue edge, forming an adherent monolayer surrounding the biopsy fragment.

C. Representative trophoblast colony after enzymatic detachment and filtration to remove residual tissue debris. Cells reorganize into well-defined adherent colonies (“islands”), characterized by tightly packed polygonal cells with clear cell–cell boundaries, typical of trophoblast epithelial organization.

3.7. Metabolic Response of Ovine Spheroids to Nutraceutical Treatment (Figure 8)

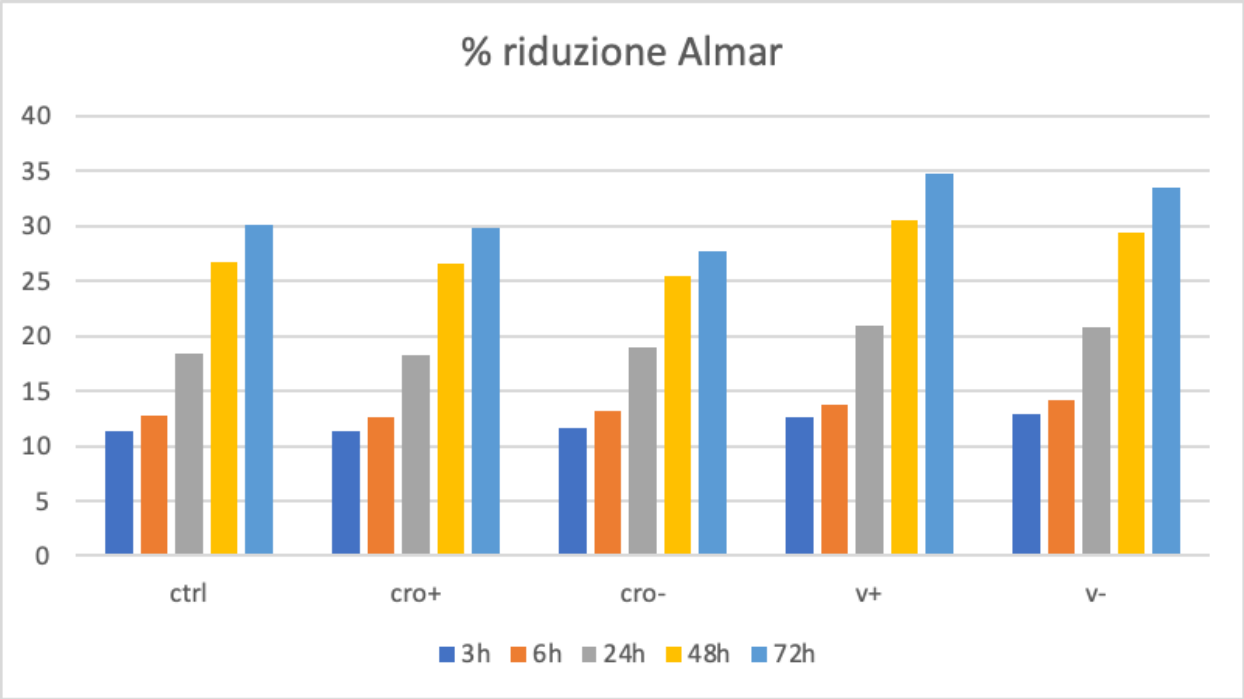

Figure 8.

Across all time points, the spheroids displayed stable metabolic profiles, and none of the treatments induced a significant decrease in viability compared to the control condition. Both concentrations of crocetin (Cro+ and Cro–) produced curves largely overlapping with the untreated spheroids, indicating no measurable cytotoxic effect at the tested doses. Verbascoside treatments showed a slightly different pattern: although differences did not reach statistical significance, the V+ group (25 µM) consistently exhibited higher Alamar Blue reduction relative to the control, suggesting a potential mild enhancement of spheroid metabolic activity.

Overall, the data indicates that the selected nutraceutical concentrations are well tolerated by ovine trophoblast spheroids, and among them, verbascoside at 25 µM appears to elicit the most favorable though not statistically significant metabolic response.

3.8. Biophysical Analysis: Mass Density, Weight, and Diameter (Figure 9)

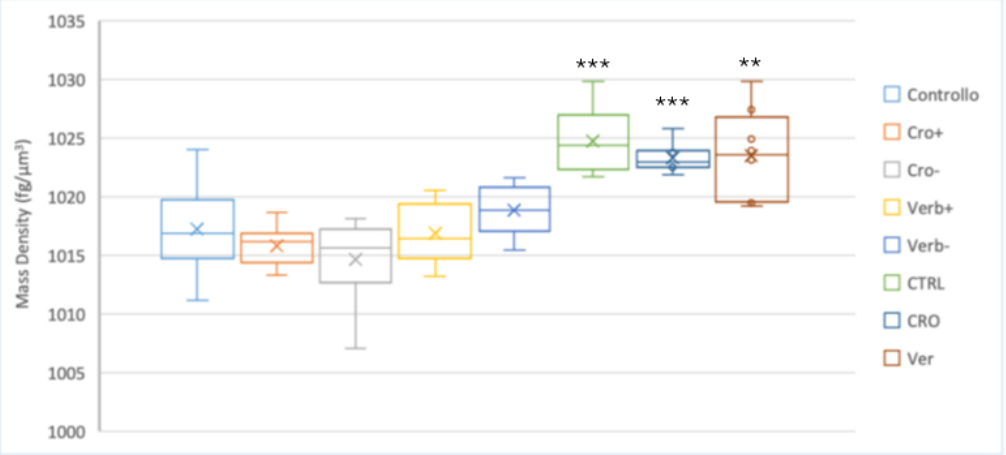

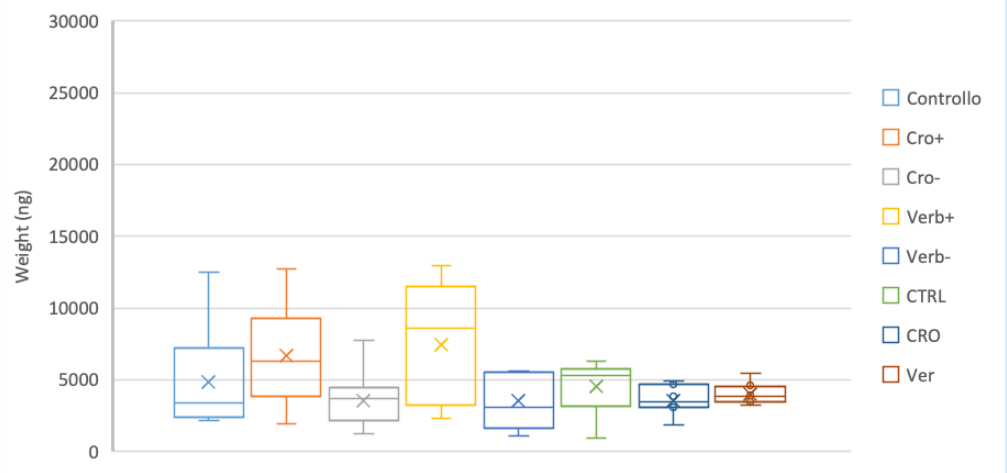

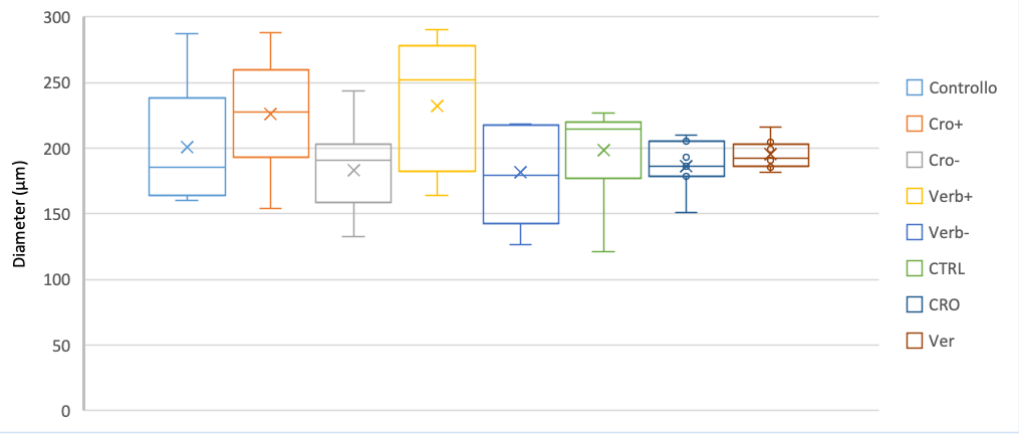

Figure 9.

The W8 analysis shown in the graphs represents the comparison of two

experimental sets: the first experiment using the hanging-drop method (experimental conditions 1–5) and the first experiment using the Agarose

aggregation system (experimental conditions 6–8). The analysis was performed on live samples after 72 hours of growth in their respective systems.

The results highlight the impact of the culture method on spheroid mass density when the initial number of cells per spheroid (2500) is kept constant. Notably, mass density is the only parameter that shows a statistically significant difference attributable to the culture system used.

Furthermore, the distribution of the samples across the three parameters mass density, weight, and diameter appears markedly more homogeneous in spheroids generated in agarose microwells compared to those produced using the hanging-drop method.

3.9. Live/Dead After Nutraceutical Exposure (Figure 10)

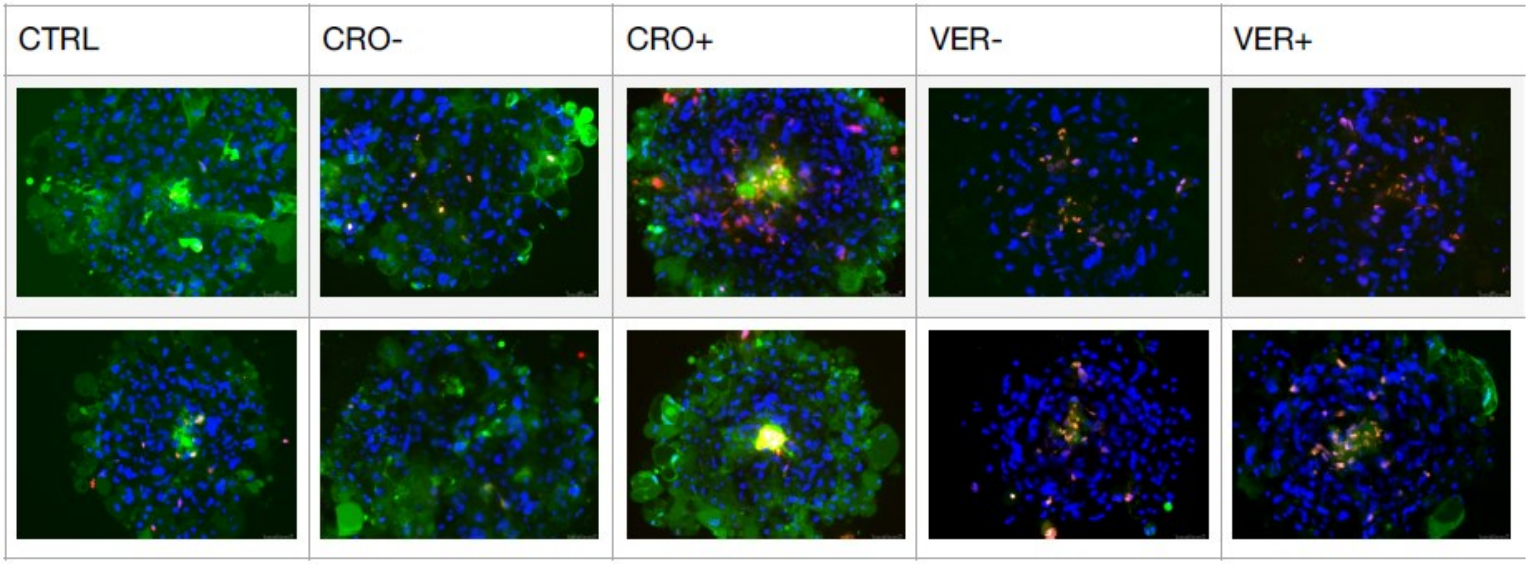

Figure 10. Live/Dead staining after 72 h of Crocetin and Verbascoside exposition. Calcein-AM (green, live cytoplasm), Hoechst 33342 (blue, all nuclei) and propidium iodide (PI, red, dead nuclei) in control (CTRL) and slow-frozen (SF) spheroids.

4. CELLviewer Prototype: Fluidic and Functional Architecture (Figure 11–12)

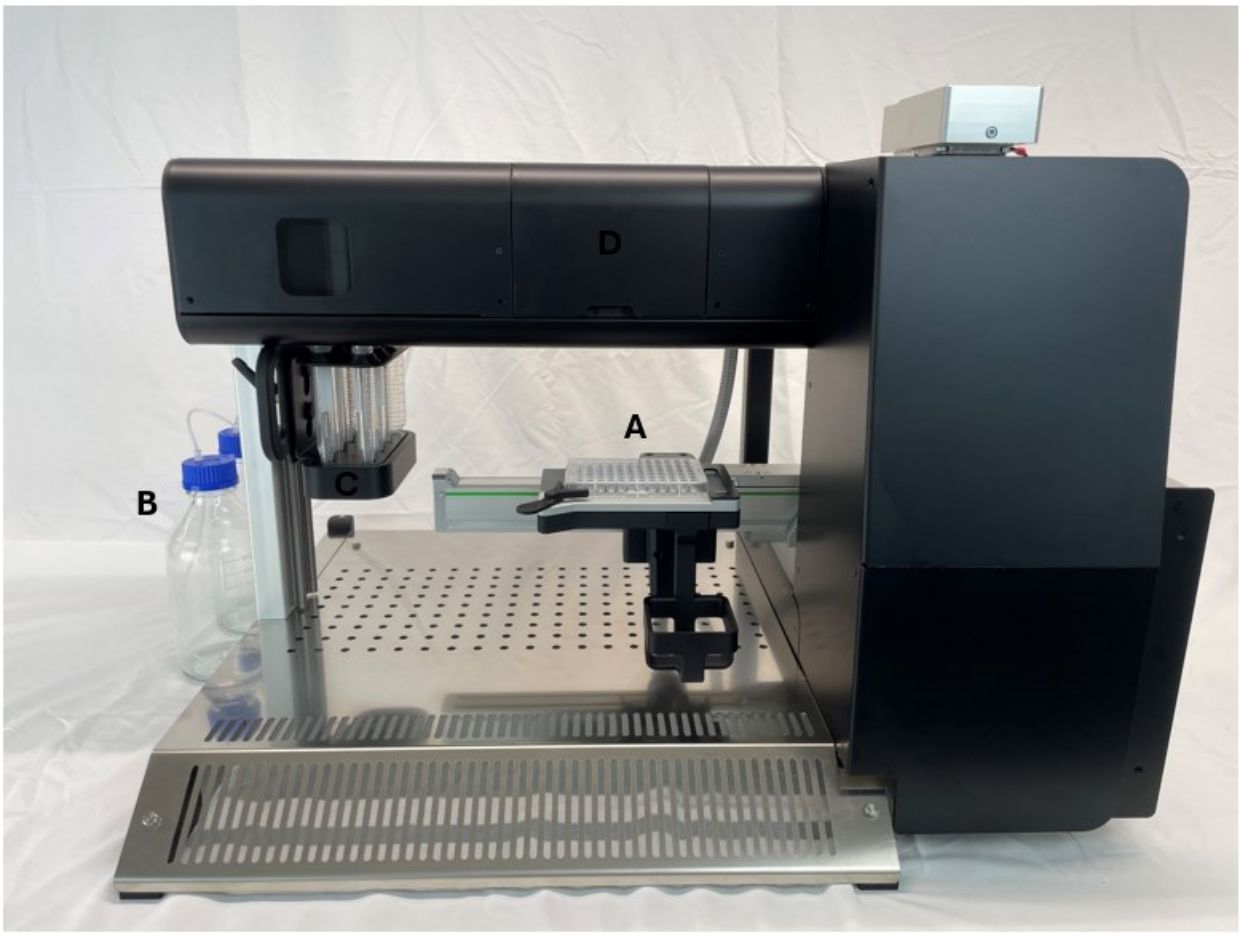

Figure 11.

The PL8 instrument is shown with its main functional components highlighted. **A** identifies the multiwell stage, which accommodates ULA 96 multiwell plates and maintains them at 37 °C through an integrated heating element, ensuring stable physiological conditions during sample handling. **B** indicates the sterilization module, composed of two dedicated reservoirs—one containing distilled water and the other a 5% bleach solution—used to automatically disinfect the entire internal fluidic circuit as well as the external buffer and chip-loading lances. **C** marks the buffer holder, a compartment designed to host up to eight independent solutions, enabling rapid and automated switching between measurement buffers, calibration media or washing solutions. **D** denotes the chip holder, the docking interface where the microfluidic analysis chip is positioned and secured during measurements, ensuring proper alignment with the optical system and stable fluidic connections.

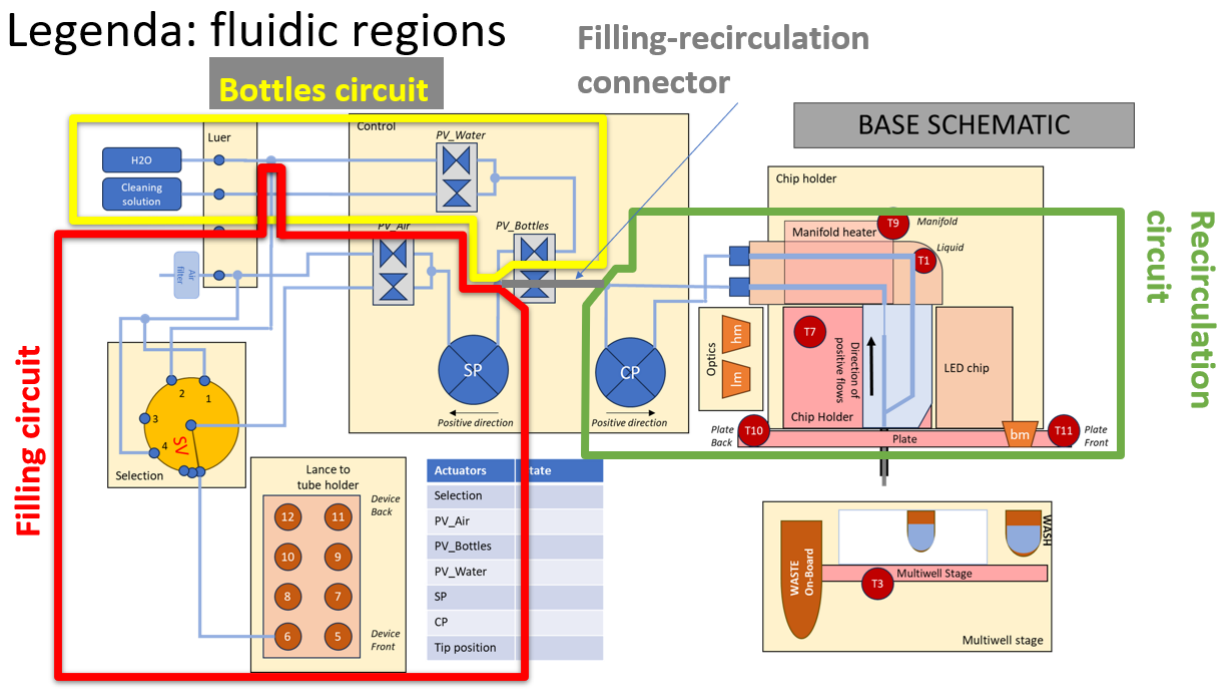

Figure 12.

The fluidic layout of the PL8 is organized into three main integrated circuits, each highlighted by a different color. The filling circuit, delineated in red, connects the eight available buffers both to the sterilization reservoirs and to the downstream fluidic path through a 12-way selection valve. This section of the system relies on the peristaltic *service pump*, which drives the movement of the selected liquid across the circuit and allows automated routing of buffers during preparation and cleaning phases. The bottle circuit, shown in yellow, is dedicated exclusively to sterilization fluids; only distilled water or 5% bleach can circulate within this closed loop, ensuring that the disinfection process remains isolated from the analytical pathways. The recirculation circuit, highlighted in green, is operated by the peristaltic *control pump* and is responsible for filling the measurement chip with the appropriate buffer while maintaining stable flow conditions during analysis. This green circuit also manages the controlled aspiration of individual spheroids or organoids directly from the growth well of the 96-well plate, guiding them into the microfluidic chip for density measurement under physiological conditions.

4.1 Sterilization results (Figure 13)

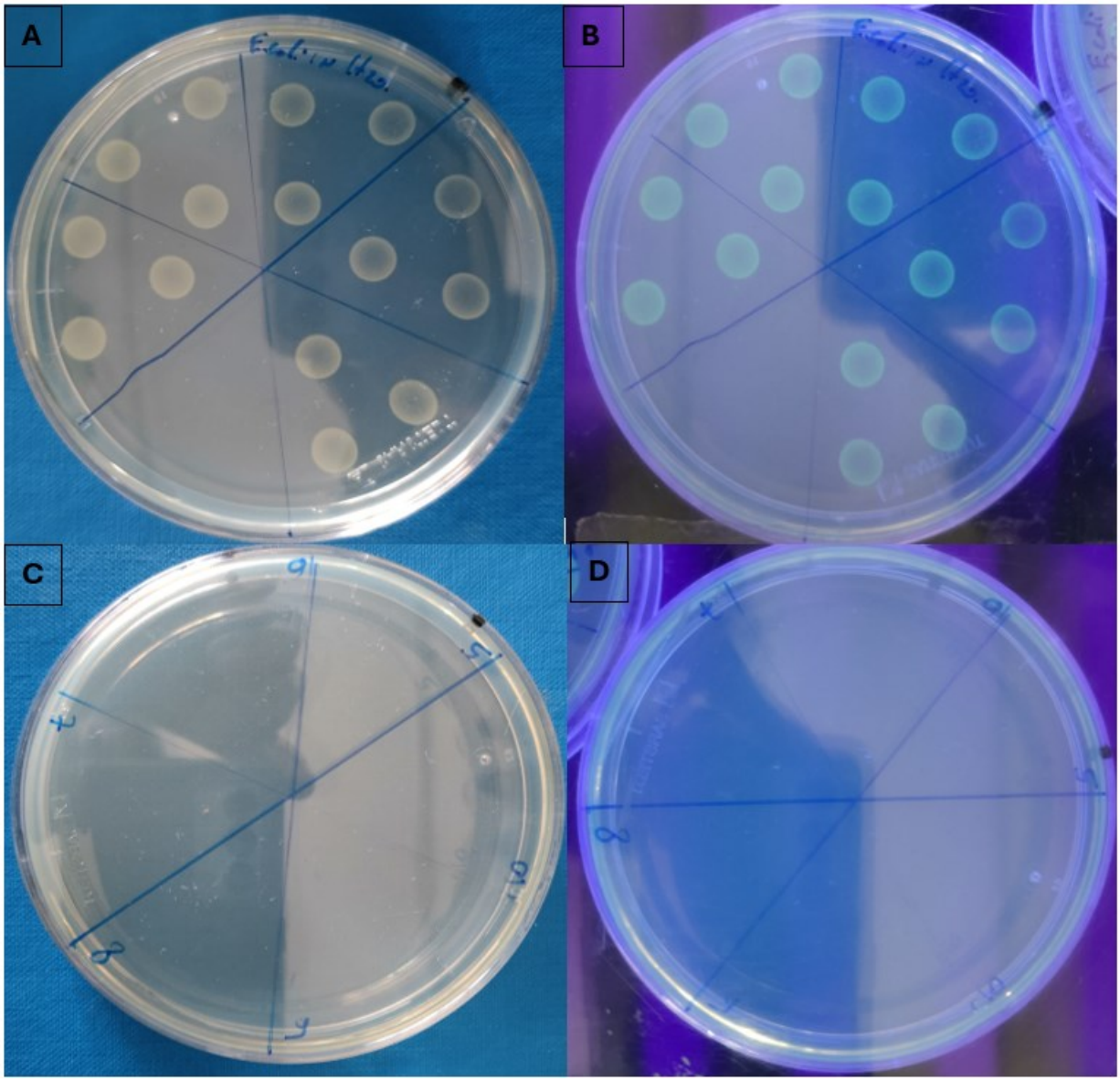

Figure 13.

The images shown in Figure 12, depict the microbiological plates used to assess the sterility of the prototype's internal fluidic system before and after the automated sterilization procedure. Each sample collected from the instrument's fluidic pathways was plated onto nutrient-rich agar, a non-selective culture medium that supports the growth of a broad range of bacteria, including GFP-positive *Escherichia coli* used in this experiment. This type of agar allows clear

visualization of colony-forming units (CFUs), enabling reliable detection of residual microbial contamination.

A. Falcon tubes 5–10 filled with GFP-positive *E. coli* suspension (10^6 CFU/mL) during the contamination phase. All tubes except one show evident bacterial growth, confirming correct loading of the microbial solution. **B**. Falcon tubes 5–10 from the contamination phase imaged under GFP fluorescence. All detected colonies exhibit strong GFP signal, indicating that bacterial growth is exclusively due to the introduced *E. coli* strain and that no environmental contamination occurred during handling. **C**. Falcon tubes 5–10 containing sterilization water collected after the automated sterilization protocol. No colony-forming units (CFUs) are detected, demonstrating complete elimination of viable bacteria. **D**. Falcon tubes 5–10 containing sterilization water imaged under GFP fluorescence. No GFP-positive colonies are observed, confirming the absence of residual *E. coli* and ruling out environmental contamination following sterilization.

5. Discussion

The results of this work demonstrate that the agarose-based microwell platform developed in this project represents a robust, scalable, and highly adaptable alternative to commercial 3D culture technologies. Existing microwell systems such as Aggrewell™ or Elplasia™ rely on rigid, non-adhesive microstructures to promote controlled aggregation, but they remain limited by fixed geometries, high manufacturing costs, and reduced flexibility in species- or experiment-specific customization. In contrast, the agarose-based system presented here exploits the intrinsic advantages of hydrogel microfabrication namely tunable stiffness, chemical inertness, and high optical transparency to generate uniform multicellular aggregates in a reproducible and cost-effective format [49].
The ability to produce hundreds of structurally homogeneous spheroids within a single disk markedly increases experimental throughput and reduces biological noise, consistent with prior reports showing that microstructured hydrogels enhance size uniformity and limit mechanical artefacts compared to polystyrene substrates [50].

Beyond its application in spheroid generation, the agarose platform revealed an unexpected but highly valuable secondary role as a short-term transport matrix. Transport of viable 3D cultures remains a largely unresolved challenge: most laboratories rely on cryopreservation or ad-hoc manual solutions that fail to ensure structural stability or metabolic preservation. Cryopreservation, while suitable for long-term storage, imposes well-documented biophysical stresses including osmotic imbalance, intracellular ice formation, and cryoprotectant toxicity that disproportionately affect compact multicellular aggregates, leading to decreased post-thaw

viability and compromised architecture [51].
The findings of this thesis show that hypothermic agarose-based stabilization enables safe transport of spheroids over 24–72 h while maintaining morphology, metabolic activity, and mass-density profiles comparable to fresh samples. This outcome is notable given that the literature on spheroid transport is extremely limited and mostly focused on organoid models or tissue slices rather than small multicellular aggregates [52]. Hydrogels such as agarose inherently provide mechanical buffering, reduced shear forces, and a hydrated microenvironment conditions analogous to hydrogel-based tissue preservation approaches described for organoids and engineered tissues [53]. By enabling robust, non-cryogenic shipment of viable spheroids, this method significantly increases the logistical flexibility of laboratories relying on 3D culture workflows.

Biophysical characterization further highlighted the strengths of this platform. Spheroids generated in agarose microwells displayed markedly narrower density distributions than those formed by the classical hanging-drop method, reflecting more homogeneous internal compaction and organization. Hanging-drops are known to be sensitive to subtle variations in droplet geometry, evaporation, and initial sedimentation dynamics, all of which amplify inter-spheroid heterogeneity [54]. The controlled geometric confinement provided by agarose microwells thus supports a more reproducible internal architecture, reinforcing the central role of microenvironmental constraints stiffness, dimensionality, and mechanical uniformity in shaping aggregate morphology and function [55].

Mass density emerged as one of the most informative parameters across all assays performed. Unlike fluorescence-based viability tests or molecular biomarkers, density integrates macromolecular crowding, hydration state, cytoplasmic viscosity, and intracellular structural organization into a single quantitative readout [56].
Differences in density correlated with metabolic activity, structural degradation, or hypoxic stress, enabling discrimination between spheroids subjected to cryopreservation, hypothermic transport, or nutraceutical exposure. This corroborates recent evidence highlighting density as a sensitive reporter of cell state, apoptosis, metabolic suppression, and cytoskeletal remodeling in multiple biological contexts [57].
Because density profiling is label-free and non-destructive, it provides a unique advantage in the analysis of 3D constructs that cannot be easily dissociated or stained without sacrificing viability.

The integration of nutraceutical molecules further validated the biological relevance of this system. Crocetin and verbascoside both recognized for their antioxidant and anti-inflammatory actions exhibited dose-dependent effects on trophoblast spheroids, including subtle increases in metabolic activity and moderate shifts in biophysical parameters. These results align with previous research demonstrating that crocetin enhances mitochondrial performance and

reduces oxidative injury in mammalian cells, while verbascoside exerts cytoprotective activity through ROS scavenging and modulation of stress-responsive pathways [58,59].
Although the responses observed in ovine spheroids did not reach statistical significance, the trends support the hypothesis that nutraceutical compounds may modulate placental cell physiology, consistent with emerging work on antioxidant supplementation in reproductive biotechnology and trophoblast models [60].

A major technological outcome of this thesis is the development of a prototype microfluidic instrument capable of performing mass-density measurements directly in 96-well plates and under physiologically relevant conditions. Unlike the commercial W8 analyzer which requires dedicated measurement buffers and imposes constraints on sample size and fragility the prototype maintains specimens at 37 °C, operates directly in culture medium, and integrates automated retrieval of spheroids using a dual-pump fluidic architecture. This enables measurement of delicate aggregates and oocytes without exposing them to non-physiological fluids or mechanical perturbations.
Calibration experiments demonstrated high concordance between this device and the W8 system, validating its suitability for longitudinal, real-time biophysical analysis. The capacity to quantify density in temperature-controlled conditions and without changing the culture medium represents a substantial methodological advancement, supporting more biologically realistic readouts and reducing assay-induced artefacts [61].

Although the primary application explored in this thesis focused on trophoblast-derived spheroids, the biophysical characterization framework developed here is not limited to multicellular aggregates. The ability of the prototype instrument to perform label-free mass-density measurements directly in physiological culture conditions opens the possibility of extending this approach to other complex biological systems.

In this context, the exploratory measurements performed on ovine oocytes, presented in Appendix A, illustrate the potential applicability of density-based biophysical analysis in reproductive biology. Oocyte quality assessment remains a major challenge in assisted reproduction, where current selection strategies rely largely on morphological criteria or invasive biochemical assays. The possibility of quantifying intrinsic physical parameters such as mass density in a non-destructive manner could provide an additional objective indicator of oocyte physiological status.

Although these observations are presented as a preliminary dataset, they highlight the broader translational potential of the biophysical platform developed in this work, suggesting that density-based characterization may represent a promising analytical tool for future applications in reproductive biotechnology.

An essential component of the instrument's development was the establishment and validation of a fully automated sterilization protocol. Ensuring sterility in closed microfluidic systems is notoriously challenging, particularly when working with live spheroids or primary cells under laminar-flow conditions. For this reason, a dedicated sterilization workflow based on 5% bleach and sterile water was implemented and validated through bacterial contamination assays. Fluidic lines, buffer reservoirs, chip-loading ports, and all internal channels were intentionally contaminated with GFP-expressing *E. coli* at 10^6 CFU/mL, followed by a 3-hour operational simulation mimicking real experimental conditions. Samples collected before and after sterilization demonstrated complete elimination of bacterial colonies, confirming the efficacy of the automated disinfection cycle. Similar sterilization validation strategies are widely adopted in industrial and biomedical microfluidic systems, as surface-adherent microorganisms can persist in valves, pumps, and dead-volume regions unless rigorous chemical and mechanical flushing protocols are applied [62,63].
Subsequent experiments performed using DMEM across six independent buffer lines confirmed the absence of post-sterilization contamination, further validating the robustness of the design for biological applications.

Overall, the integrated results of this thesis highlight the power of combining agarose-based 3D culture, hypothermic stabilization, nutraceutical modulation, and advanced microfluidic biophysical analysis within a unified technological framework. The agarose microwell system offers reproducibility and scalability; the transport method provides practical inter-laboratory mobility; the density-based analytical workflow supplies quantitative, label-free biological insight; and the new prototype instrument expands the experimental reach of biophysical cytometry.
Importantly, the prototype instrument developed during this project is now actively used by CellDynamics partners, including IRST (Istituto Scientifico Romagnolo per lo Studio e la Cura dei Tumori, Forlì), the Department of Pharmacy and Biotechnology (FaBiT) of the University of Bologna, and the Department of Biomedical Sciences – Histology and Human Embryology Unit of the University of Bologna. Its deployment in these research centers underscores the translational potential and technological maturity of the system, highlighting its relevance for ongoing work in oncology, microbiology, and developmental biology.

Together, these advancements reinforce the central theme of this thesis: the convergence of bioengineering, microfluidics, and veterinary cell biology enables novel methodological ecosystems capable of supporting next-generation 3D culture research across species, tissues, and experimental paradigms.

6. Conclusions

This doctoral project provides a comprehensive technological and biological framework for the standardized generation, preservation, and biophysical characterization of three-dimensional (3D) cellular systems, with a specific focus on ovine trophoblast models. Through the integration of agarose microstructured scaffolds, hypothermic transport strategies, nutraceutical modulation, and advanced mass-density analysis, the work establishes a unified methodological ecosystem capable of addressing key limitations that have historically constrained the reproducibility and translational value of 3D cultures.

The agarose-based microwell platform proved to be a robust and versatile system for producing highly uniform spheroids across multiple cell types. Its inert surface chemistry, defined microarchitecture, and mechanical stability enabled controlled aggregation and minimized inter-spheroid variability an improvement over traditional scaffold-free systems such as hanging drops, which often suffer from heterogeneity and mechanical inconsistency. Furthermore, the unexpected effectiveness of agarose as a short-term transport matrix represents a valuable contribution to the field. The ability to immobilize spheroids within a protective hydrogel layer ensured minimal mechanical stress during simulated shipment and preserved metabolic function and structural integrity for up to 72 hours, offering a practical alternative to conventional cryopreservation for short-distance biological transfer.

Cryopreservation experiments confirmed the intrinsic limitations of slow-freezing protocols when applied to compact 3D aggregates. Despite maintaining overall morphology, cryopreserved spheroids exhibited significant reductions in metabolic activity and increased PI-positive staining, consistent with intracellular damage associated with ice crystal formation and cryoprotectant toxicity. In contrast, spheroids stored under hypothermic transport conditions preserved viability and density profiles comparable to fresh samples, reinforcing the suitability of agarose-based stabilization as a gentler preservation strategy.

The biophysical analyses conducted using both the commercial W8 analyzer and the custom-developed microfluidic density-measurement device demonstrated that mass density is a sensitive and integrative biomarker capable of detecting subtle biological alterations not easily captured by traditional microscopy or metabolic assays. Density measurements differentiated not only between culture systems (agarose vs. hanging drop) but also between developmental stages of ovine oocytes and between spheroids subjected to transport, cryopreservation, or nutraceutical treatments. The successful validation of the custom instrument expands future analytical capabilities by enabling temperature-controlled, high-throughput, and physiologically relevant measurements on fragile samples. Beyond its application to trophoblast spheroids, the biophysical characterization approach developed in this thesis may also have relevant implications for reproductive biology. The exploratory density measurements performed on

ovine oocytes, presented in Appendix A, illustrate how intrinsic physical parameters such as mass density could contribute to the objective assessment of gamete physiological status. Since current strategies for oocyte selection largely rely on morphological evaluation, the possibility of integrating non invasive biophysical measurements may represent a promising direction for future research in reproductive biotechnology and assisted reproduction technologies.

The nutraceutical experiments further confirmed the biological applicability of the system. In JAR cells, dose–response screening revealed that intermediate concentrations of crocetin and verbascoside supported or enhanced metabolic activity, with Cro3 (54.2 µM) and Ver3 (25 µM) identified as optimal candidates. When applied to ovine trophoblast spheroids, these compounds exhibited no cytotoxic effects and, in the case of verbascoside, a mild but consistent trend toward increased metabolic activity, suggesting potential protective roles under physiological or stress conditions.

Taken together, these findings highlight the strength of integrating engineering principles with biological experimentation. The methodologies developed in this thesis not only improve the reproducibility and transportability of 3D systems but also provide new quantitative tools for assessing viability, structural organization, and treatment response in veterinary and reproductive models. This work establishes the foundation for future studies on 3D culture standardization, hypothermic preservation of organoids and gametes, and the application of biophysical metrics to reproductive biotechnology. It also underscores the value of ovine trophoblast spheroids as a species-specific in vitro platform for exploring placental physiology, environmental influences, and potential therapeutic interventions.

Overall, the thesis advances both technological innovation and biological understanding, contributing a versatile, scalable, and analytically rich platform for the next generation of 3D cell culture research.

Appendix A

Analysis of Ovine Oocytes

This appendix presents the detailed methodology, imaging documentation, and quantitative biophysical measurements of ovine oocytes analyzed using the W8 Physical Cytometer. The dataset includes germinal vesicle (GV) oocytes of high (C+) and low (C–) morphological quality, as well as metaphase-II (MII) oocytes collected after in vitro maturation.

Importantly, this work represents the first application of a terminal-velocity–based biophysical analysis to ovine oocytes, providing direct measurements of mass density, weight, and diameter in intact gametes. Unlike conventional morphological classification, which is inherently subjective and limited to visual assessment, mass-density profiling offers a quantitative and objective descriptor of oocyte quality, capturing intracellular organization, cytoplasmic compaction, macromolecular distribution, and hydration state.

Although not central to the primary aims of the thesis, these measurements provide significant comparative insight into the relationship between oocyte morphology and biophysical state. Differences between C+, C–, and MII oocytes highlight how maturation and cytoplasmic quality translate into measurable physical parameters establishing a foundation for future applications of label-free biophysical cytometry in reproductive biology, oocyte selection, and assisted reproduction in domestic species.

The samples analyzed at W8 consist of 3 groups of ovine oocytes in biological triplicates, divided as follow:

- **C+**. Oocytes in germinal vesicle stage (GV), more suitable for maturation due to the presence of a complete cumulus layer, uniform cytoplasm, the absence of vacuoles, uniformity in the distribution of lipids and uniformity of the zona pellucida;
- **C-**. Oocytes in GV, less suitable for maturation due to the presence of alterations in the cumulus layer, non-uniform cytoplasm, lipid polarization and vacuolization
- **MII**. Oocytes in metaphase II after IVM;

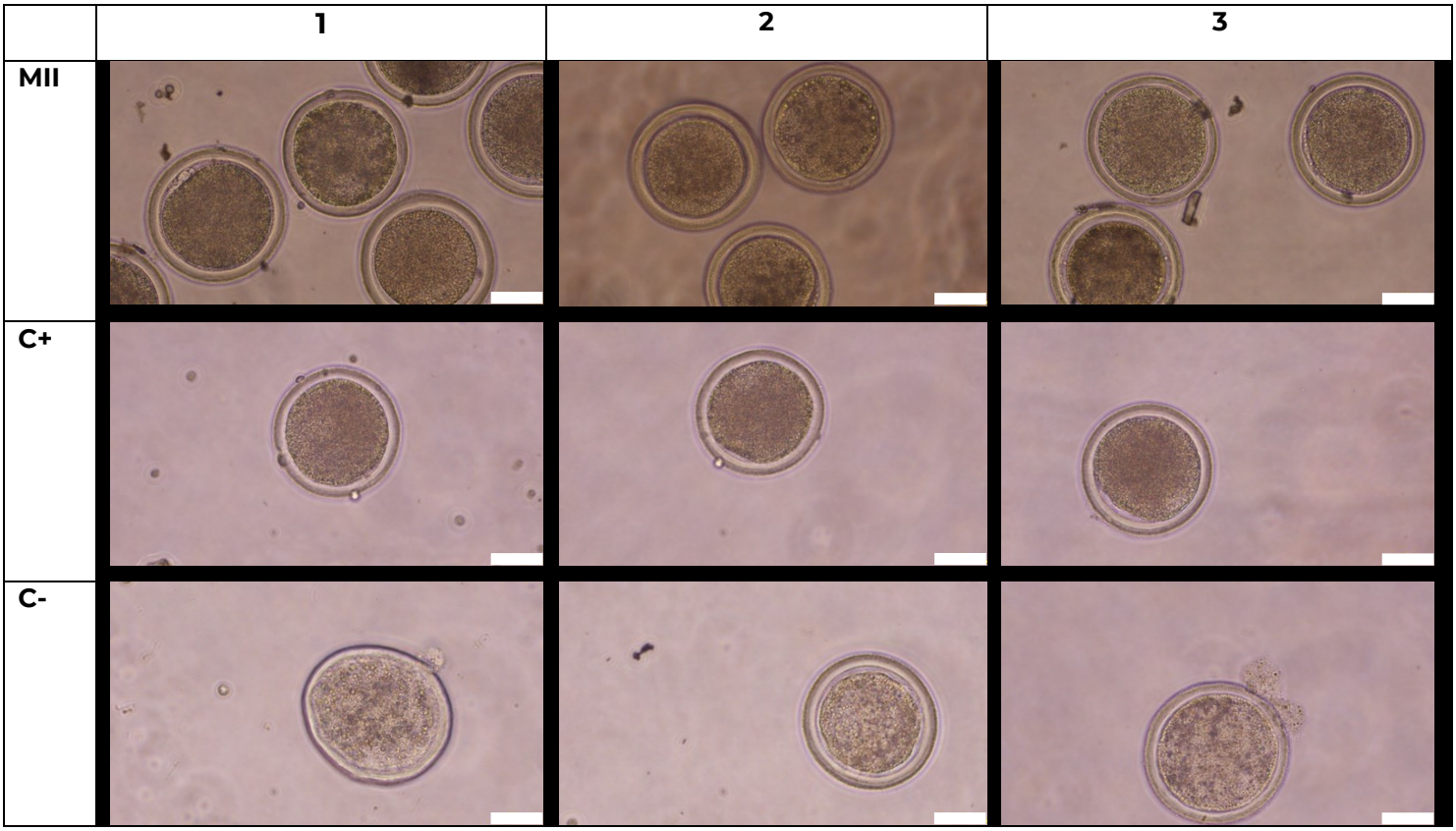

Figure 14. Phase contrast image acquired prior to analysis at W8 of MII, C+, C- oocytes. Oocytes **MII** after 24h of maturation in IVM culture medium and after the decumulation of the granulosa cells, show the polar body, a compact and defined cytoplasm, absence of alterations in the zona pellucida; Oocytes **C+** recovered from ovine ovary by scraping, immediately decumulated by the granulosa cells, they show the germinal vesicle, a compact and defined cytoplasm, uniformity in the lipid composition and absence of alterations in the pellucid zone; Oocytes **C-** recovered from ovine ovary by scraping and immediately decumulated by granulosa cells, show alterations in the zona pellucida, vacuolized cytoplasm, poor lipid presence and polarization. The white bar indicated **50µm.**

Samples	Mass Density (fg/µm3)	Weight (ng)	Diameter (µm)	Oocytes / Condition
MII-1	1027.9 ± 2.7	1082 ± 166	126 ± 7	12
MII-2	1028.8 ± 2.8	996 ± 185	122 ± 8	13
MII-3	1027.0 ± 1.2	1138 ± 102	128 ± 4	8
Oocytes 1 C+	1023.2 ± 2.6	1254 ± 291	133 ± 13	9
Oocytes 1 C-	1018.1 ± 2.5	1490 ± 173	141 ± 6	12
Oocytes 2 C+	1020.4 ± 2.1	1037 ± 237	124 ± 9	12

Oocytes 2 C-	1016.6 ± 1.9	1151 ± 282	129 ± 11	9
Oocytes 3 C+	1023.4 ± 4.3	1145 ± 243	128 ± 9	9
Oocytes 3 C-	1016.8 ± 1.6	1295 ± 141	134 ± 5	15

Table 1.

Show the average of the mass density, weight and diameter values for each group analyzed.

W8. Biophysical Analysis (Figure 15)

A.

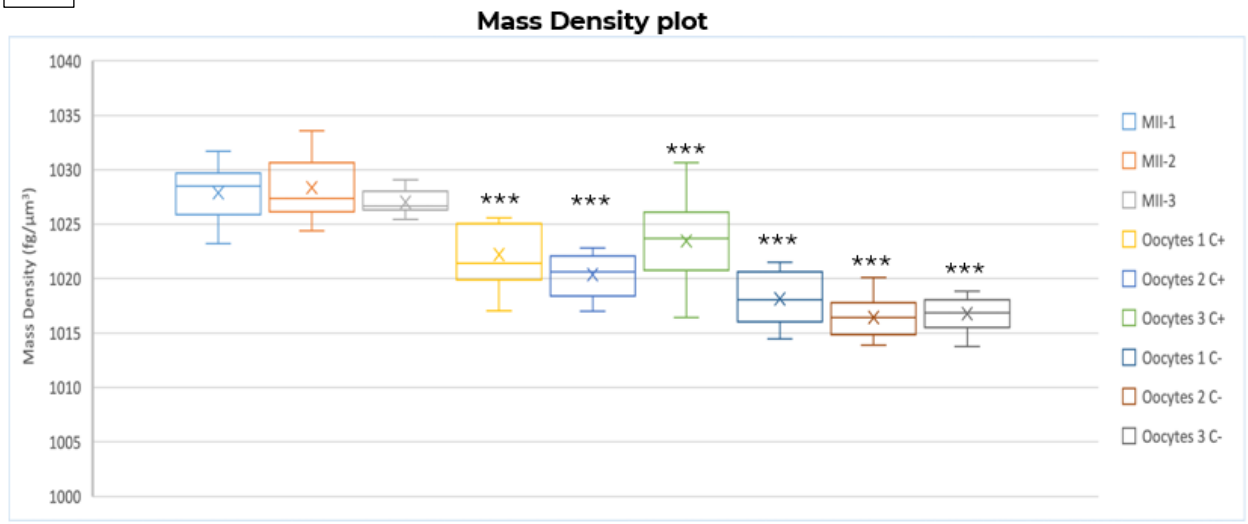

B.

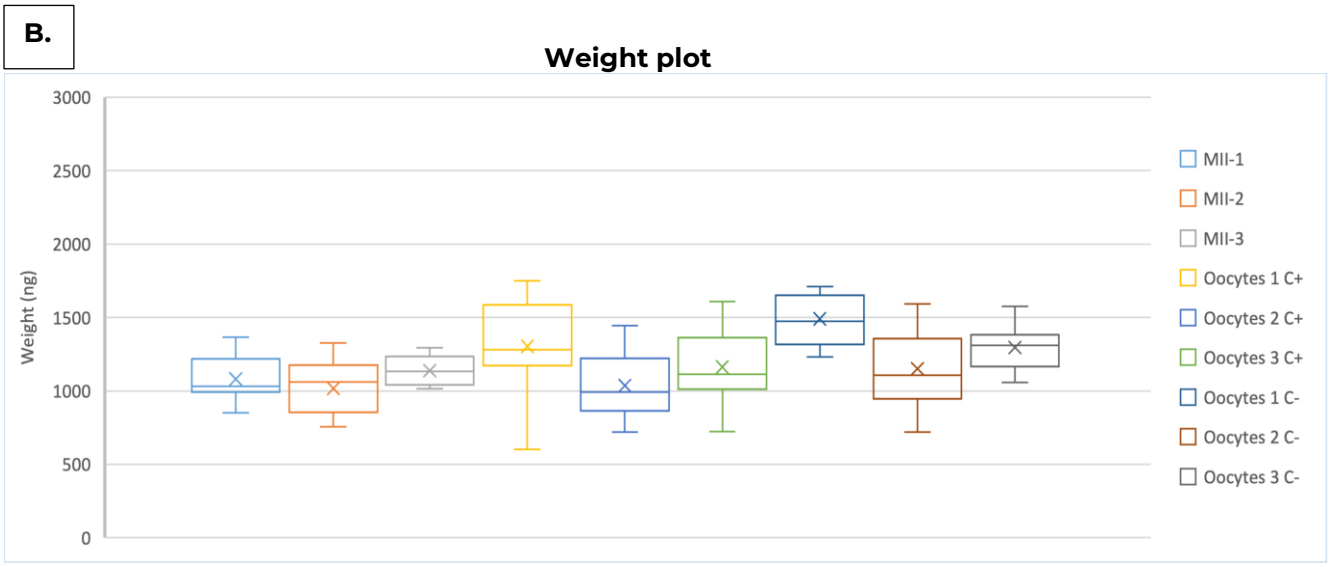

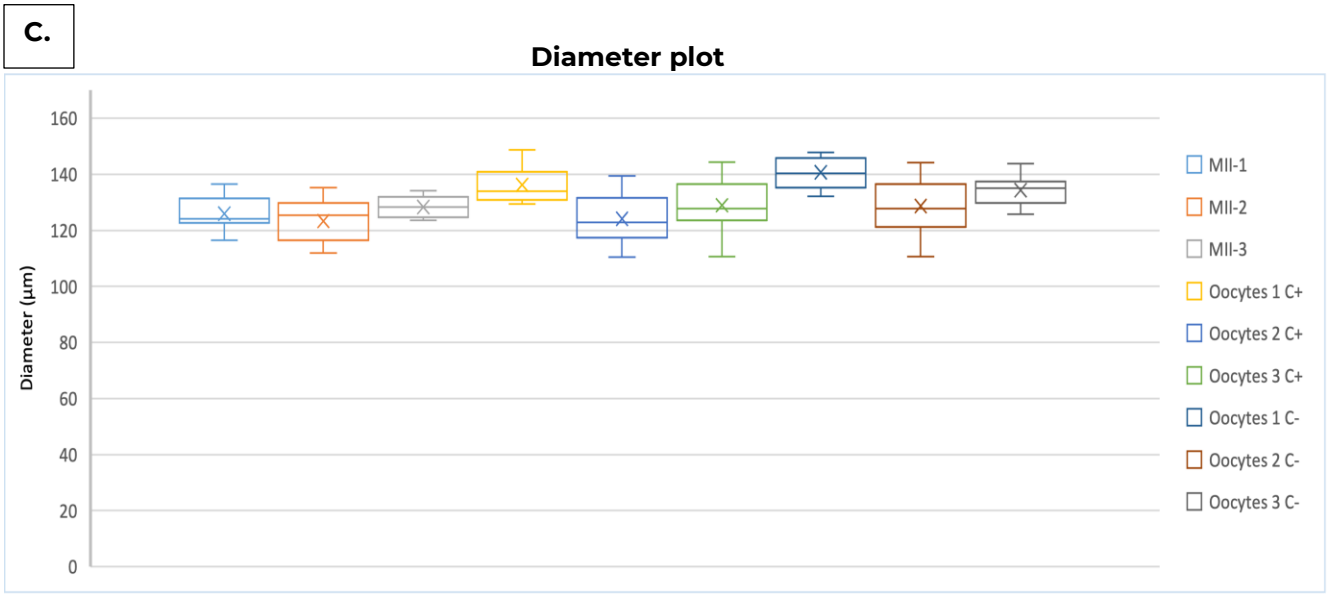

Figure 15.

Measurement of mass density **(A)**, weight **(B)** and diameter **(C)** of ovine oocytes.

The results show significant differences in particular in mass density, comparing the three groups, it can be noted that the density is on average higher in oocytes in MII and decreases in group C + and decreases further in C-; this may reflect the initial selection of oocytes in GV, in which in C- we have a less compact cytoplasm and a lower lipid mass than in C +; while the highest oocyte mass density values in MII may coincide with the complex interaction of several important intracellular, paracrine, and structural factors within the oocyte maturation, that include lipid accumulation, rearrangement of mitochondria, alignment of cortical granules along the plasma membrane, increase of the number of the ribosomes as well as changes in the activity of cell cycle regulatory enzymes MAPK (Mitogen-Activated Protein Kinase) and MPF (Maturation-Promoting Factor; all factors that together are able to increase compaction and density of the oocyte.

7. References

1. Edmondson R, Broglie JJ, Adcock AF, Yang L. Three-dimensional cell culture systems and their applications in drug discovery and cell-based biosensors. *Assay Drug Dev Technol*. 2014;12(4):207–218. doi:10.1089/adt.2014.573
2. Antoni D, Burckel H, Josset E, Noel G. Three-dimensional cell culture: A breakthrough in vivo. *Int J Mol Sci*. 2015;16(3):5517–5527. doi:10.3390/ijms16035517
3. Yamada KM, Cukierman E. Modeling tissue morphogenesis and cancer in 3D. *Cell*. 2007;130(4):601–610. doi:10.1016/j.cell.2007.08.006
4. Ravi M, et al. 3D cell culture systems: Advantages and applications. *J Cell Physiol*. 2015;230(1):16–26. doi:10.1002/jcp.24683
5. Thoma CR, et al. 3D cultures in oncology research. *Nat Rev Cancer*. 2014;14(10):563–580. doi:10.1038/nrc3791
6. Ranga A, et al. 3D niche microenvironments for stem cell fate. *Nat Rev Mol Cell Biol*. 2014;15(12):761–769. doi:10.1038/nrm3905
7. Dupont S, et al. Role of YAP/TAZ in mechanotransduction. *Nature*. 2011;474(7350):179–183. doi:10.1038/nature10137
8. Friedrich J, et al. Spheroid-based drug screen: Challenges and opportunities. *Adv Drug Deliv Rev*. 2009;61(8):785–795. doi:10.1016/j.addr.2009.03.005
9. Ferraz MAMM, Rho HS, Hemerich D, Henning HHW, van Tol HTA, Hölker M, Besenfelder U, Mokry M, Vos PLAM, Stout TAE, Le Gac S, Gadella BM. An oviduct-on-a-chip provides an enhanced in vitro environment for zygote genome reprogramming. *Nature Communications*. 2018;9(1):4934. doi:10.1038/s41467-018-07119-8
10. Pinto B, Henriques AC, Silva PMA, Bousbaa H. Three-dimensional spheroids as in vitro preclinical models for cancer research. *Pharmaceutics*. 2020;12(12):1186. doi:10.3390/pharmaceutics12121186. PMID:33291351; PMCID:PMC7762220.
11. Yamauchi N, Yamada O, Takahashi T, Imai K, Sato T, Ito A, Hashizume K. A three-dimensional cell culture model for bovine endometrium: regeneration of a multicellular spheroid using ascorbate. *Placenta*. 2003;24(2–3):258–269. doi:10.1053/plac.2002.0901.
12. Haeger JD, Hambruch N, Dilly M, Froehlich R, Pfarrer C. Formation of bovine placental trophoblast spheroids. *Cells Tissues Organs*. 2011;193(4):274–284. doi:10.1159/000320544. PMID:20975254.
13. Rossant J, Cross JC. Placental development: lessons from mouse mutants. *Nature Reviews Genetics*. 2001;2(7):538–548. doi:10.1038/35080570
14. Roberts RM, Green JA, Schulz LC. The evolution of the placenta. *Reproduction*. 2016;152(5):R179–R189. doi:10.1530/REP-16-0325
15. Lonergan P, Fair T. The ART of studying early embryo development: progress and challenges in ruminant embryo culture. *Theriogenology*. 2014;81(1):49–55. doi:10.1016/j.theriogenology.2013.09.021
16. Vinci M, et al. Advances in establishment and analysis of three-dimensional tumor spheroid-based functional assays for target validation and drug evaluation. *BMC Biol*. 2012;10:29. doi:10.1186/1741-7007-10-29
17. Baker BM, Chen CS. Deconstructing the third dimension: How 3D microenvironments alter cellular cues. *J Cell Sci*. 2012;125:3015–3024. doi:10.1242/jcs.079509

18. Kelm JM, et al. Method for generation of homogeneous multicellular tumor spheroids applicable to a wide variety of cell types. *Biotechnol Bioeng*. 2003;83:173–180. doi:10.1002/bit.10655
19. Chan HF, et al. Rapid formation of multicellular spheroids in double-emulsion droplets with controllable microenvironment. *Sci Rep 3, 3462 (2013). https://doi.org/10.1038/srep03462*

20. Abbott A. Cell culture: biology's new dimension. *Nature*. 2003;424:870–872. doi:10.1038/424870a
21. Napolitano AP, Dean DM, Man AJ, Youssef J, Ho DN, Rago AP, Lech MP, Morgan JR. Scaffold-free three-dimensional cell culture utilizing micromolded nonadhesive hydrogels. *Biotechniques*. 2007;43(4):494–500. doi:10.2144/000112591. PMID:18019341.
22. Normand V, Lootens DL, Amici E, Plucknett KP, Aymard P. New insight into agarose gel mechanical properties. *Biomacromolecules*. 2000;1(4):730–738. doi:10.1021/bm005583j. PMID:11710204.
23. Unsworth BR, Lelkes PI. Growing tissues in microgravity. *FASEB J*. 1998;12:2–9. doi:10.1096/fasebj.12.2.2
24. Huh D, et al. Reconstituting organ-level functions on a chip. *Science*. 2010;328:1662–1668. doi:10.1126/science.1188302
25. Engler AJ, et al. Matrix elasticity directs stem cell lineage specification. *Cell*. 2006;126:677–689. doi:10.1016/j.cell.2006.06.044
26. Normand V, Lootens DL, Amici E, Plucknett KP, Aymard P. New insight into agarose gel mechanical properties. *Biomacromolecules*. 2000;1(4):730–738. doi:10.1021/bm005583j. PMID:11710204.
27. Gong X, Lin C, Cheng J, Su J, Zhao H, Liu T, Wen X, Zhao P. Generation of multicellular tumor spheroids with microwell-based agarose scaffolds for drug testing. *PLoS One*. 2015;10(6):e0130348. doi:10.1371/journal.pone.0130348. PMID:26090664; PMCID:PMC4474551.
28. an C, Wang DA. Macroporous hydrogel scaffolds for three-dimensional cell culture and tissue engineering. *Tissue Eng Part B Rev*. 2017;23(5):451–461. doi:10.1089/ten.TEB.2016.0465. PMID:28067115.
29. Yeh J, Ling Y, Karp JM, Gantz J, Chandawarkar A, Eng G, Blumling J 3rd, Langer R, Khademhosseini A. Micromolding of shape-controlled, harvestable cell-laden hydrogels. *Biomaterials*. 2006;27(31):5391–5398. doi:10.1016/j.biomaterials.2006.06.005. PMID:16828863.
30. Baust JG, Snyder KK, Van Buskirk R, Baust JM. Integrating molecular control to improve cryopreservation outcome. *Biopreserv Biobank*. 2017;15(2):134–141. doi:10.1089/bio.2016.0119.
31. Karlsson JOM, Toner M. Long-term storage of tissues by cryopreservation: critical issues. *Biomaterials*. 1996;17(3):243–256. doi:10.1016/0142-9612(96)85562-0
32. Gao D, Critser JK. Mechanisms of cryoinjury in living cells. *ILAR Journal*. 2000;41(4):187–196. doi:10.1093/ilar.41.4.187
33. Best BP. Cryoprotectant toxicity: facts, issues, and questions. *Rejuvenation Research*. 2015;18(5):422–436. doi:10.1089/rej.2014.1656
34. Belzer FO, Southard JH. Principles of solid-organ preservation by cold storage. *Transplantation*. 1988;45(4):673–676. doi:10.1097/00007890-198804000-00001
35. Tibbitt MW, Anseth KS. Hydrogels as extracellular matrix mimics for 3D cell culture. *Biotechnology and Bioengineering*. 2009;103(4):655–663. doi:10.1002/bit.22361
36. Luby-Phelps K. The physical chemistry of cytoplasm and its influence on cell function: an update. *Molecular Biology of the Cell*. 2013;24(17):2593–2596. doi:10.1091/mbc.E12-08-0617
37. Ellis RJ. Macromolecular crowding: an important but neglected aspect of the intracellular environment. *Curr Opin Struct Biol*. 2001;11(1):114–119. doi:10.1016/S0959-440X(00)00172-X

38. Popescu G. *Quantitative Phase Imaging of Cells and Tissues*. McGraw-Hill; 2011.
39. Cermak N, Olcum S, Feijó Delgado F, et al. High-throughput measurement of single-cell growth rates using serial microfluidic mass sensor arrays. *Nature Biotechnology*. 2016;34(10):1052–1059. doi:10.1038/nbt.3666
40. Cristaldi DA, Sargenti A, Bonetti S, et al. A reliable flow-based method for the accurate measurement of mass density, size and weight of live 3D tumor spheroids. *Cells*. 2019;8(10):1224. doi:10.3390/cells8101224
41. Edmondson R, Broglie JJ, Adcock AF, Yang L. Three-dimensional cell culture systems and their applications in drug discovery and cell-based biosensors. *Assay and Drug Development Technologies*. 2014;12(4):207–218. doi:10.1089/adt.2014.573
42. Grimes DR, Kelly C, Bloch K, Partridge M. A method for estimating the oxygen consumption rate in multicellular tumour spheroids. *Journal of the Royal Society Interface*. 2014;11(92):20131124. doi:10.1098/rsif.2013.1124
43. Wooding FBP, Burton GJ. *Comparative Placentation: Structures, Functions and Evolution*. Springer; 2008. doi:10.1007/978-3-540-74099-8
44. Davenport KM, Ortega MS, Johnson GA, Seo H, Spencer TE. Implantation and placentation in ruminants. *Animal*. 2023;17(S1):100796. doi:10.1016/j.animal.2023.100796
45. Turco MY, Gardner L, Kay RG, et al. Trophoblast organoids as a model for maternal–fetal interactions during human placentation. *Nature*. 2018;564(7735):263–267. doi:10.1038/s41586-018-0753-3
46. Knöfler M, Haider S, Saleh L, Pollheimer J, Gamage TKJB, James J. Human placenta and trophoblast development: key molecular mechanisms and model systems. *Cellular and Molecular Life Sciences*. 2019;76(18):3479–3496. doi:10.1007/s00018-019-03104-6
47. Rizos D, Fair T, Papadopoulos S, Boland MP, Lonergan P. Developmental, qualitative, and ultrastructural differences between ovine and bovine embryos produced in vivo or in vitro. *Molecular Reproduction and Development*. 2002;62(3):320–327. doi:10.1002/mrd.10138
48. Gilchrist RB, Lane M, Thompson JG. Oocyte-secreted factors: regulators of cumulus cell function and oocyte quality. *Human Reproduction Update*. 2008;14(2):159–177. doi:10.1093/humupd/dmm040
49. Tang Y, Liu J, Chen Y. Agarose multi-wells for tumour spheroid formation and anti-cancer drug test. *Microelectronic Engineering*. 2016;158:1–6. doi:10.1016/j.mee.2016.03.009
50. Baker BM, Chen CS. Deconstructing the third dimension. J Cell Sci. 2012;125:3015–3024.
51. Baust JM, Corwin W, Snyder KK, Van Buskirk R, Baust JG. Cryopreservation: evolution of molecular-based strategies. *Advances in Experimental Medicine and Biology*. 2016;951:13–29. doi:10.1007/978-3-319-45457-3_2
52. Pegg DE. Principles of cryopreservation. *Methods in Molecular Biology*. 2007;368:39–57. doi:10.1007/978-1-59745-362-2_3
53. Lancaster MA, Knoblich JA. Organogenesis in a dish: modeling development and disease using organoid technologies. *Science*. 2014;345(6194):1247125. doi:10.1126/science.1247125
54. Foty R. A simple hanging drop cell culture protocol for generation of 3D spheroids. *Journal of Visualized Experiments*. 2011;(51):2720. doi:10.3791/2720
55. Discher DE, Janmey P, Wang YL. Tissue cells feel and respond to the stiffness of their substrate. *Science*. 2005;310(5751):1139–1143. doi:10.1126/science.1116995

56. Ellis RJ. Macromolecular crowding: an important but neglected aspect of the intracellular environment. *Current Opinion in Structural Biology*. 2001;11(1):114–119. doi:10.1016/S0959-440X(00)00172-X

57. Phillips R, Kondev J, Theriot J, Garcia HG. *Physical Biology of the Cell*. 2nd ed. Garland Science; 2012. doi:10.1201/9781134111589

58. Ochiai M, Nagao T. Crocetin prevents oxidative stress-induced cell death. J Nutr Biochem. 2019;66:46–54.

59. Marčetić M, Bufan B, Drobac M, Antić Stanković J, Arsenović Ranin N, Milenković MT, Božić DD. Multifaceted biological properties of verbascoside/acteoside: antimicrobial, cytotoxic, anti-inflammatory, and immunomodulatory effects. *Antibiotics*. 2025;14(7):697. doi:10.3390/antibiotics14070697

60. Colapietro A, Mancini A, D'Alessandro AM, Festuccia C. Crocetin and crocin from saffron in cancer chemotherapy and chemoprevention. *Anti-Cancer Agents in Medicinal Chemistry*. 2019;19(1):38–47. doi:10.2174/1871520619666181231112453

61. Ko J, Lee J. Advanced microfluidic systems with temperature modulation for biological applications. *Biomicrofluidics*. 2025;19(3):031301. doi:10.1063/5.0251893

62. Zhang R, Huang J, Xie F, Wang B, Chu M, Wang Y, Li H, Wang W, Zhang H, Wu W, Li Z. Microfluidic sterilization. *Biomicrofluidics*. 2014;8(3):034119. doi:10.1063/1.4882776

63. Ugwu CN, Ezeibe EN, Emencheta SC, Nwagwu CS, Ogbonna KO, Ejiofor CV, Onugwu AL, Berebon DP, Attama AA. Biofilms: structure, resistance mechanism, emerging control strategies, and applications. *Materials Advances*. 2025. doi:10.1039/D5PM00094G